Journal of Medicinal Chemistry

Article

Discovery of Multi-Target Agents Active as Broad-Spectrum Antivirals and Correctors of Cystic Fibrosis Transmembrane Conductance Regulator (CFTR) for Associated Pulmonary Diseases

Sabrina Tassini, Liang Sun, Kristina Lanko, Emmanuele Crespan, Emily Langron, Federico Falchi, Miroslava Kissova, Jorge I. Armijos-Rivera, Leen Delang, Carmen Mirabelli, Johan Neyts, Marco Pieroni, Andrea Cavalli, Gabriele Costantino, Giovanni Maga, Paola Vergani, Pieter LEYSSEN, and Marco Radi

J. Med. Chem., **Just Accepted Manuscript** • DOI: 10.1021/acs.jmedchem.6b01521 • Publication Date (Web): 25 Jan 2017

ACS Publications

Journal of Medicinal Chemistry is published by the American Chemical Society. 1155 Sixteenth Street N.W., Washington, DC 20036

Discovery of Multi-Target Agents Active as Broad-Spectrum Antivirals and Correctors of Cystic Fibrosis Transmembrane Conductance Regulator (CFTR) for Associated Pulmonary Diseases

Sabrina Tassini,[a] Liang Sun,[b] Kristina Lanko,[b] Emmanuele Crespan,[c] Emily Langron,[d] Federico Falchi,[e,f] Miroslava Kissova,[c] Jorge I. Armijos-Rivera,[c] Leen Delang,[b] Carmen Mirabelli,[b] Johan Neyts,[b,*] Marco Pieroni,[a] Andrea Cavalli,[e,f] Gabriele Costantino,[a] Giovanni Maga,[c] Paola Vergani,[d] Pieter Leyssen,[b] and Marco Radi[a,*]

[a]P4T Group, Dipartimento di Scienze degli Alimenti e del Farmaco, Università degli Studi di Parma, Viale delle Scienze, 27/A, 43124 Parma, Italy;

[b]Laboratory of Virology and Experimental Chemotherapy, Rega Institute for Medical Research, KU Leuven, Minderbroedersstraat 10, 3000, Leuven, Belgium;

[c]Istituto di Genetica Molecolare, IGM-CNR, Via Abbiategrasso 207, 27100 Pavia, Italy;

[d]Department of Neuroscience, Physiology and Pharmacology, University College London, Gower Street, WC1E 6BT London, UK;

[e]CompuNet, Istituto Italiano di Tecnologia, Via Morego 30, I-16163 Genova, Italy;

[f]Department of Pharmacy and Biotechnology, University of Bologna, Via Belmeloro 6, I-40126 Bologna, Italy.

KEYWORDS: PI4KIIIβ, F508del-CFTR, broad-spectrum antivirals, enterovirus, cystic fibrosis, multi-target.

ABSTRACT

Enteroviruses (EVs) are among the most frequent infectious agents in humans worldwide and represent the leading cause of upper respiratory tract infections. No drugs for the treatment of EV infections are currently available. Recent studies have also linked enterovirus infection with pulmonary exacerbations, especially in cystic fibrosis (CF) patients, and the importance of this link is probably underestimated. The aim of this work was to develop a new class of multi-target agents active both as broad-spectrum antivirals and as correctors of the F508del-CFTR folding defect responsible for >90% of CF cases. We report herein the discovery of the first small-molecules able to simultaneously act as correctors of the F508del-CFTR folding defect and as broad-spectrum antivirals against a panel of enteroviruses representative of all major species.

INTRODUCTION

Enteroviruses (EVs) are positive-sense single stranded RNA viruses, classified into 12 species, including four human enterovirus species (EV-A to EV-D), three species of human rhinoviruses (RV-A to RV-C) and five enterovirus species that only infect animals.[1] EVs are responsible for a great variety of clinical manifestations, especially in young children, which may result in life-threatening neurological complications (e.g. encephalitis, meningitis and poliomyelitis-like paralysis).[2-4] Furthermore, RV infections are now considered one of the major causes of acute exacerbations in chronic pulmonary diseases like asthma, chronic

obstructive pulmonary disorder (COPD) and cystic fibrosis (CF) in children and adults.[5] Physicians pay particular attention to patients that already suffer from respiratory diseases, such as CF or asthma, as they could be particularly affected by an additional enterovirus infection.[6] An increasing number of studies also suggest that respiratory viruses, in particular enterovirus and rhinovirus, contribute significantly to CF pulmonary exacerbations, hospitalization, decreased lung function and predisposition to bacterial colonization.[7] The mechanistic link between viral infections and deterioration of CF lung function is not fully understood and their impact is probably underestimated, especially in young children.[8] Despite their high clinical and socioeconomic impact, to date there is no approved antiviral therapy for the prophylaxis and/or the treatment of enterovirus infections, and the management of patients is currently limited to symptomatic treatment and supportive care. Therefore, there is an unmet need for broad-spectrum antiviral drugs as a rapid defense strategy against enterovirus infections and virus-related exacerbations.

Nowadays, host factors are considered as very attractive targets for the development of antiviral drugs because they are unlikely to mutate and develop resistance in response to therapy.[9] Moreover, since viruses belonging to the same genus or family usually share the same cellular pathways for replication, targeting a host factor may allow the development of effective broad-spectrum antiviral compounds.[10] Although some toxicity risks may be expected from inhibiting a host factor, it should be kept in mind that most drugs currently used in therapy target host proteins with excellent therapeutic outcomes and acceptable safety profiles. In particular, it has been well documented that the host lipid kinase phosphatidylinositol 4-kinase IIIβ (PI4KIIIβ) is critical for RNA replication of several enteroviruses.[11-14] PI4KIIIβ belongs to the phosphatidylinositol 4-kinases (PI4Ks) that synthesize phosphatidylinositol 4-phosphate (PI4P) from phosphatidylinositol (PI). PI4P is involved in signaling and cellular trafficking mainly at the Golgi and trans-Golgi network

(TGN), it contributes to defining the characteristics of plasma membranes and it activates a variety of ion channels, including CFTR.[15-18] Four PI4K isoforms have been identified in mammals, classified as type II (PI4KIIα and PI4KIIβ) or type III (PI4KIIIα and PI4KIIIβ) based on their primary sequences and catalytic properties.[19] Type III PI4Ks are hijacked by several ss(+)RNA viruses (especially from *Flaviviridae*, *Picornaviridae* and *Coronaviridae* families) to remodel cellular membranes and generate PI4P lipid-enriched organelles specialized for viral replication.[20]

A few PI4KIIIβ inhibitors with antiviral activity against a panel of picornaviruses have been reported recently (Figure 1).[21-23] Generally, chemical inhibition of PI4KIIIβ does not influence cell viability.[24] One possible explanation might be that while the small amounts of PI4P produced by other PI4K isoforms could be enough to support cell trafficking and signaling, it would not be sufficient to sustain viral RNA synthesis.[20] A major aim in the development of PI4KIIIs inhibitors is to achieve selective inhibition of the α or β isoforms. Among known PI4KIIIs inhibitors, compound **1** (PIK93) is about 100-fold more potent against the PI4KIIIβ isoform, although it also has detectable activity towards PI3-kinases.[25,26]

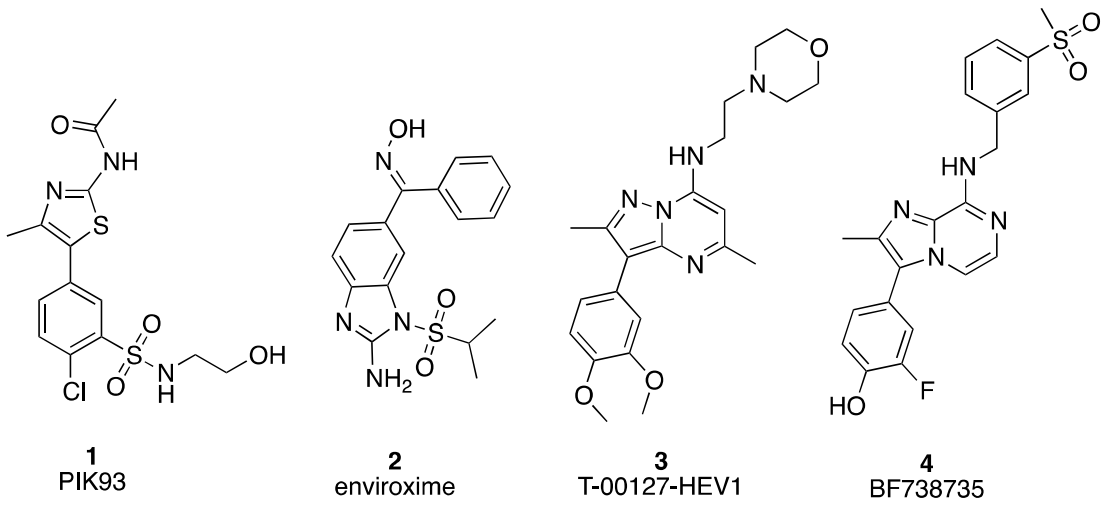

Figure 1. Representative PI4KIIIβ inhibitors.

Considering the growing need for novel broad-spectrum antivirals to fight emerging epidemics and the link between respiratory viruses and pulmonary exacerbation in cystic fibrosis patients, our aim was the development of a new class of multi-target agents active both as broad-spectrum antivirals (by targeting PI4KIIIβ) and as correctors of the F508del-CFTR folding defect responsible for >90% of CF cases. We here report the discovery of the first small-molecule compounds able to simultaneously act as moderately efficacious correctors of the F508del-CFTR folding defect and broad-spectrum antivirals against a panel of enteroviruses (linked to CF pulmonary exacerbations).

RESULTS AND DISCUSSION

Drug repurposing and polypharmacology are two very attractive approaches in modern drug discovery. The first offers the possibility of recycling known drugs or advanced drug candidates developed for a different disease. The second results in simultaneous action on different targets/diseases with a single, rationally designed drug.[27,28] In particular, polypharmacology aims at producing multi-target agents whose interference with multiple biochemical pathways offers an advantage - in terms of drug load, efficacy and safety - over combination therapy. This approach is well suited to complex diseases that generally require the simultaneous administration of many different drugs. Considering the increasing number of reports on the connection between enterovirus infections and pulmonary exacerbations in CF patients, we reasoned that an ideal drug candidate for such closely related diseases might be a multi-target agent able to act, at the same time, on proteins/pathways implicated in enterovirus replication (PI4KIIIβ) and on F508del-CFTR biogenesis. At the beginning of this work, the X-ray structures of the above targets were not available for a structure-based study. We therefore developed a PI4KIIIβ homology model to be used for the design of PI4KIIIβ inhibitors, selecting those whose chemical scaffolds resemble known CFTR

correctors/potentiators. The structure of the complex of PI3Kγ with compound **1** (PDB ID: 2CHZ)[26] has been used to build the homology model of PI4KIIIβ by using Prime software (see methods): this structure shows an identity of 30%, a positive of 52% and a score of 322. The presence of **1** in the structure of PI3Kγ allowed us to identify its likely binding site in PI4KIIIβ and hypothesize its binding mode. A 10 ns molecular dynamics simulation on the modeled PI4KIIIβ protein containing compound **1** was performed using the software Desmond.[29] In the latter (equilibrated) part of the trajectory (last 2 ns) 100 frames were extracted and clusterized on the basis of RMSD. Five clusters were obtained. All PI4Kβ inhibitors available in Pubchem[30] were docked in the compound **1** binding site of each cluster and the frame with the best correlation between docking score and enzymatic activity was selected for virtual screening. A high-throughput docking (HTD) approach was then applied to the compound **1** binding site in our PI4KIIIβ model to identify high affinity hits within the Asinex database collection.[31] Compound selection was based on the ranking score and visual inspection of the PI4KIIIβ catalytic site, but also took into account the 2D similarity to known CFTR correctors/potentiators. Thirteen commercially available compounds (**5-17**, Figure 2), four of which (**6**, **11**, **16**, **17**) resemble known CFTR correctors,[32,33] were selected for biological investigation. These computational results were confirmed on the recently released crystal structure of PI4KIIIβ co-crystallized with compound **1**, and this structure (PDB ID: 4D0L) was used for all the following simulations.[34]

These commercially available compounds were then tested both against the PI4KIIIβ enzyme and in a virus-cell-based replication assay. In particular these compounds were evaluated for antiviral activity against a panel of enteroviruses that are representative of all major species: enterovirus group A (EV71), group B (coxsackievirus B3, CVB3, and echovirus 11, ECHO11), group C (poliovirus 1, PV1), group D (enterovirus 68, EV68), rhinovirus group A (RV02) and rhinovirus group B (RV14). Among the selected compounds,

only the bithiazole **17** showed activity in cell-free and cell-based assays and possesses a chemical scaffold (the bithiazole) of a known family of CFTR correctors (Figure 2).[33,35] Compound **17** was therefore selected as a promising starting point for further structure-based optimization.

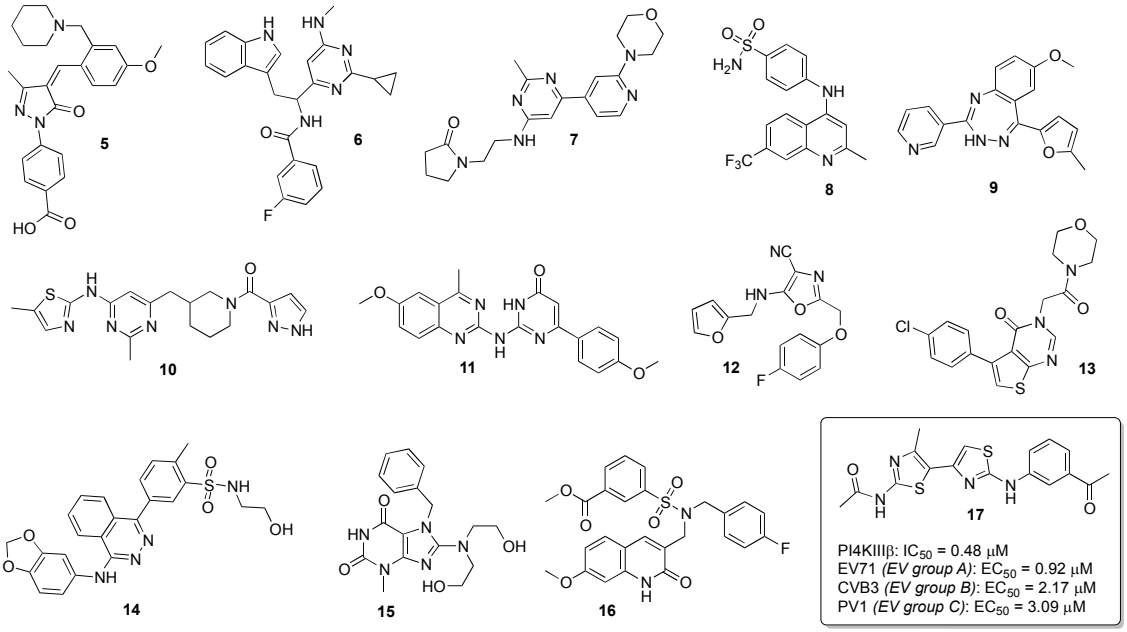

Figure 2. Chemical structure of compounds selected by virtual screening and activity profile of the hit compound **17**.

Chemistry

Compound **17** was initially resynthesized to validate the biological activity of the commercial sample and to set up a synthetic protocol for its chemical diversification starting from cheap and commercially available building blocks (Scheme 1).

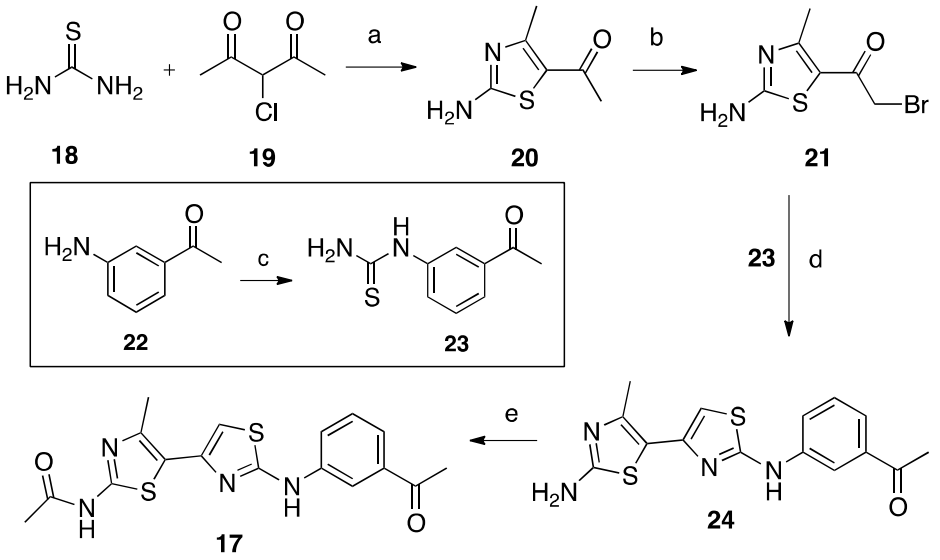

Scheme 1. Reagents and conditions: (a) EtOH, reflux, 12 h, 95%; (b) 48% aqueous HBr, Br_2, 1,4-dioxane, 60 °C, 3 h, 90%; (c) (i) benzoyl isothiocyanate, DCM, rt, 12 h, (ii) NaOH 1N, THF, reflux, 3 h, 72%; (d) EtOH, reflux, 1 h, 84%; (e) acetyl chloride, Et_3N, DCM, rt, 15 h, 77%.

Thiourea **18** was condensed with 3-chloro-2,4-pentadione **19** in refluxing ethanol to afford 1-(2-amino-4-methylthiazol-5-yl)ethanone **20** in nearly quantitative yield,[36] followed by bromination α to the carbonyl to give compound **21**. The subsequent condensation of intermediate **21** with 1-(3-acetylphenyl)thiourea **23** gave bithiazole **24** that was finally N-acetylated to obtain the desired compound **17**. Thiourea **23** was synthesized by reaction of 3'-aminoacetophenone **22** with benzoyl isothiocyanate, followed by a basic hydrolysis to remove the benzoyl group.[37]

Docking studies on compound **17** (see Molecular modeling and SAR section) showed a pattern of interactions within the ATP-binding pocket of PI4KIIIβ very similar to that of the reference compound **1**. The proposed binding mode of **17** suggested that two main portions of this molecule could be functionalized to explore the biologically relevant chemical space: *i)*

the 2-amino group on the 4-methylthiazole ring (left part) and, *ii*) the phenyl ring (right part). We first explored the chemical space around the left part of compound **17**, introducing bulkier groups and urea/thiourea functions in place of the acetamide moiety. The intermediate **24** represents in fact an advanced intermediate that could be easily functionalized on the 2-amino group to give a series of functionalized derivatives (**25a-g** and **26a-d)** (Scheme 2).

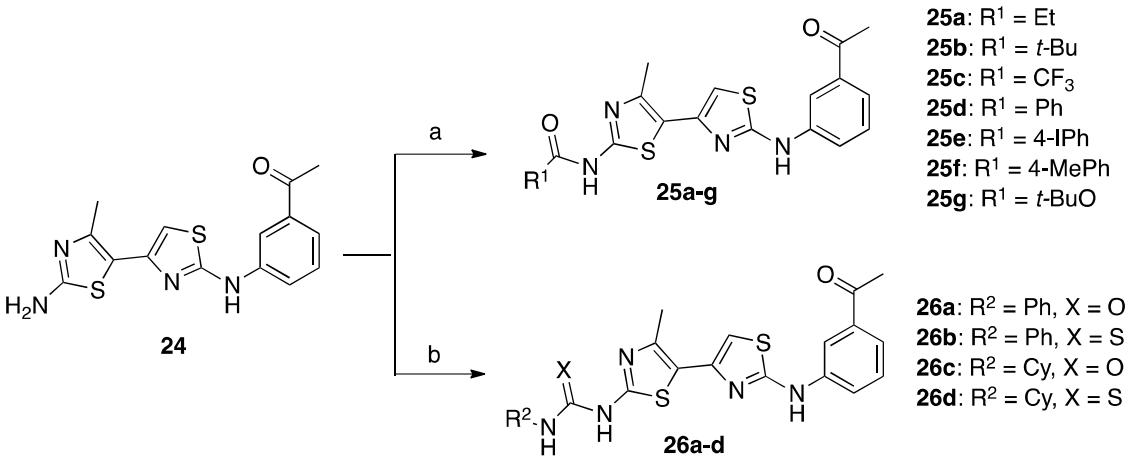

Scheme 2. Reagents and conditions: (a) method A (for **25a-c**), R^1COCl (for **25a,b**) or $(R^1CO)_2O$ (for **25c**), Et_3N, DCM, rt, 12-15 h, 65-80%; method B (for **25d-f**) R^1COCl, Et_3N, DCM, reflux, 15 h, 65-75%; method C (for **25g**), $(R^1CO)_2O$, Et_3N, DMF, 50 °C, 12 h, 63%; (b) R^2NCX, pyridine, reflux, 12-18 h, 52-69%.

Compound **24** was first reacted with different acyl chlorides or anhydrides to obtain compounds **25a-g**, while the urea/thiourea derivatives **26a-d** were synthesized by reacting **24** with the appropriate isocyanates/isothiocyanates. We also decided to replace the acetamide moiety of compound **17** with chain-extended ureidic groups for the SAR development. Unfortunately, the synthesis of compounds **30a,b** following the approach described above would have required very expensive isocyanates. Thus, an alternative synthetic approach was used for the synthesis of **30a,b** (Scheme 3): starting from 1-(2-amino-4-methylthiazol-5-yl)ethanone **20**, reaction with diphenyl carbonate gave good yields of the desired phenyl

carbamate **27** that reacted readily with the appropriate amines to give the urea intermediates **28a,b**.[38] Similar to the synthesis of compound **17**, the bromination α to the carbonyl and the subsequent condensation of intermediates **29a,b** with the 1-(3-acetylphenyl)thiourea **23**, gave the desired compounds **30a,b**.

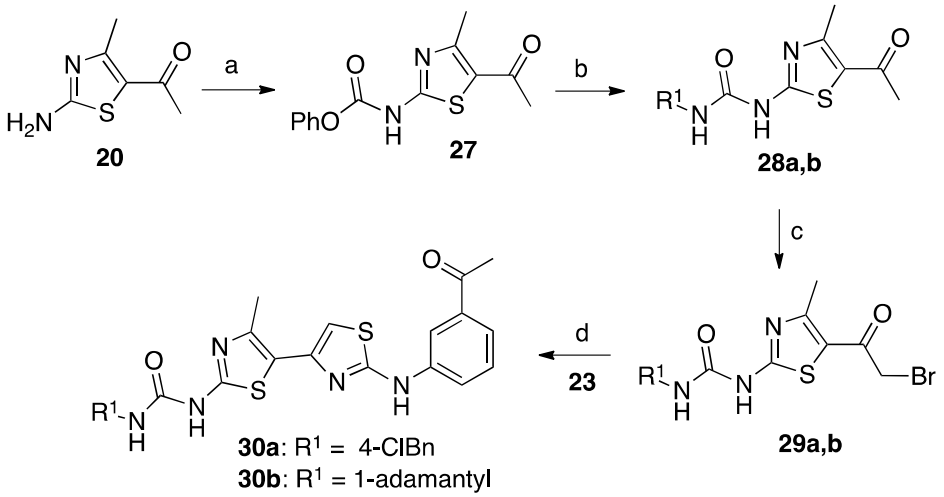

Scheme 3. Reagents and conditions: (a) diphenyl carbonate, NaH, DMF, rt, 30 min, 67%; (b) 4-chlorobenzylamine (for **28a**) or 1-adamantylamine (for **28b**), THF, 50 °C, 5-6 h, 61-93%; (c) 48% aqueous HBr, Br_2, 1,4-dioxane, 60 °C, 3 h, 88-92%; (d) EtOH, reflux, 1 h, 78-83%.

We next explored the right part of compound **17**, keeping the 2-acetamido group on the left part of the molecule unchanged and modifying the substitution pattern of the phenyl ring on the right part. Since the acetamide moiety on the left part of the molecule was conserved, intermediate **20** was conveniently acetylated before the bromination α to the carbonyl (Scheme 4). Final compounds **35a-d** were quickly obtained in good yields by reacting **32** with substituted thioureas **34a-d**, previously synthesized from the corresponding amines **33a-d.**

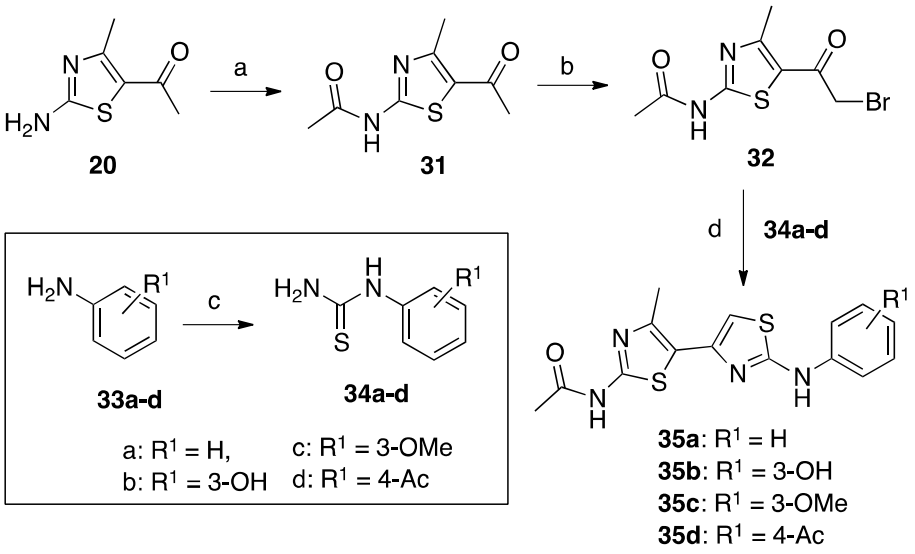

Scheme 4. Reagents and conditions: (a) acetyl chloride, pyridine, THF/DCM, 0 °C, 3 h, 87%; (b) Br_2, 1,4-dioxane, 50 °C, 22 h, 84%; (c) (i) benzoyl isothiocyanate, DCM, rt, 12 h, (ii) NaOH 1N, THF, reflux, 2 h, 72-78%; (d) EtOH, reflux, 1h, 71-85%.

Then we decided to modify the central bithiazole scaffold of the hit compound **17**, to get additional SAR information. As described in Scheme 5, we first introduced an imidazole ring by reacting intermediate **21**with the 1-(3-acetylphenyl)guanidine **36**, obtained by treating 3'-aminoacetophenone **22** with cyanamide.[39] Compound **38** was thus synthesized by acylation of the intermediate **37** with acetyl chloride.

A scaffold hopping approach (FAF-drugs2 server)[40] was also employed to identify alternatives to the bithiazole scaffold: among the molecules proposed by the software, the asymmetrical N,N'-diarylthiourea scaffold was considered the most promising on the basis of its synthetic accessibility and the antiviral activity of some closely related analogues reported in the literature.[41] Intermediate **41** was easily obtained by addition of 3'-aminoacetophenone **22** to 3-nitrophenyl isothiocyanate **39**, followed by reduction of the nitro group with iron powder in acidic ethanol (Scheme 6). The subsequent acylation of the amino group led to final compounds **42a,b**.

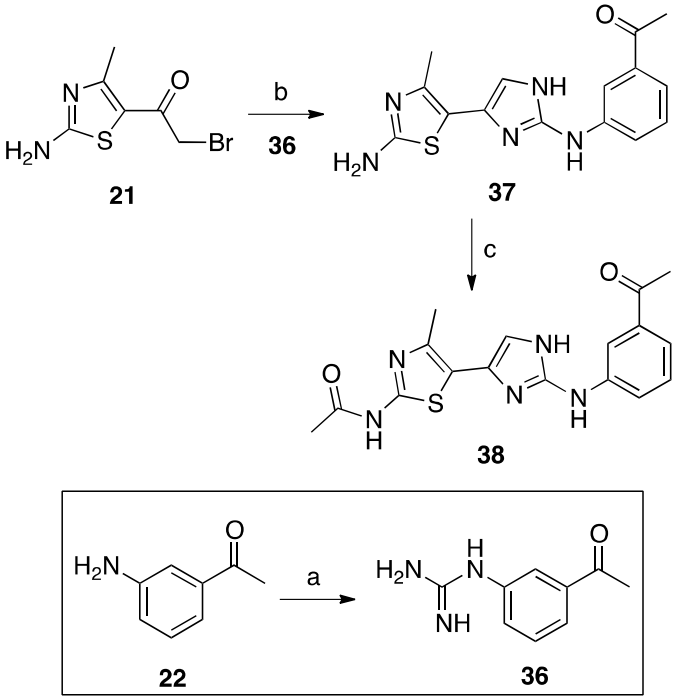

Scheme 5. Reagents and conditions: (a) cyanamide, HNO_3, $EtOH/H_2O$, reflux, 24 h, 73%; (b) Et_3N, EtOH, reflux, 12 h, 82%; (c) acetyl chloride, Et_3N, DCM, rt, 8 h, 47%.

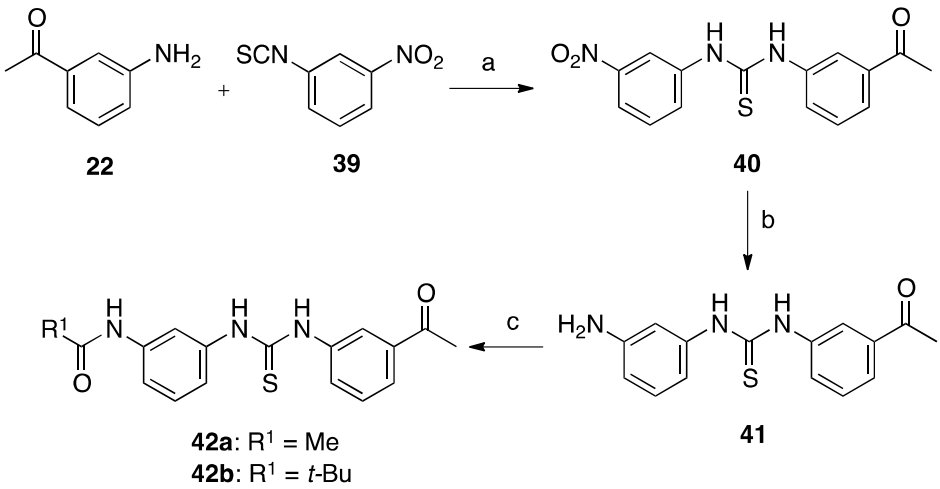

Scheme 6. Reagents and conditions: (a) DCM, rt, 18 h, 88%; (b) Fe, HCl, EtOH, reflux, 2 h, 75%; (c) acetyl chloride (for **42a**) or trimethylacetyl chloride (for **42b**), pyridine, THF, rt, 2 h, 67-69%.

Moreover we noted high chemical similarity between compound **17** and compound **46**, a known inhibitor of DC-SIGN (dendritic cell (DC)-specific intercellular adhesion molecule-3 grabbing nonintegrin).[42] The role of DC-SIGN in the binding and transmission of different pathogens, including enteroviruses, has been well investigated.[43] So we decided to evaluate the antiviral effect of compound **46** in a virus-cell-based assay and its activity on PI4KIIIβ. As described in Scheme 7, compound **46** was synthesized following the procedure previously reported for compound **17**.

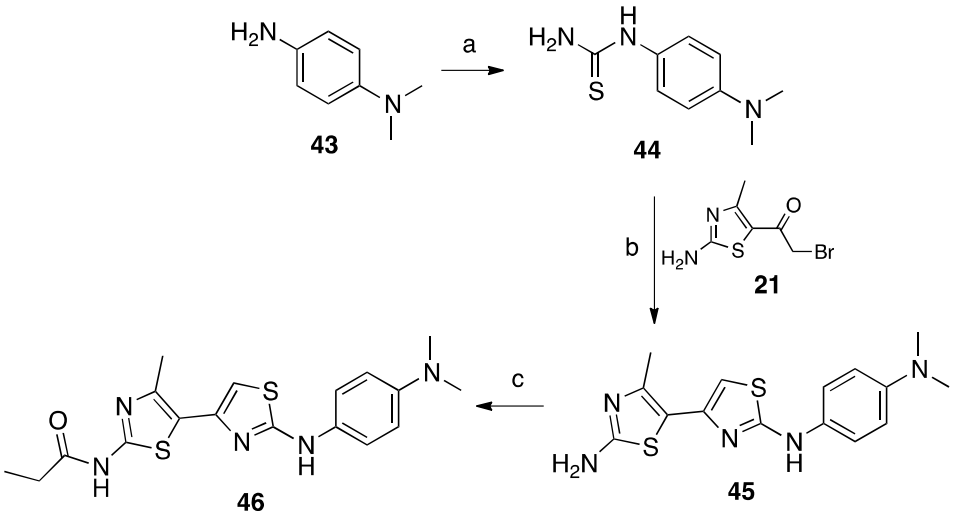

Scheme 7. Reagents and conditions: (a) (i) benzoyl isothiocyanate, DCM, rt, 12 h, (ii) NaOH 1N, THF, reflux, 3 h, 80%; (b) EtOH, reflux, 30 min, 77%; (c) propionyl chloride, Et_3N, DCM, rt, 8 h, 68%.

Finally, we decided to prepare two compounds (related to the hit **17**) known in the CFTR field to evaluate the potential role of the CFTR channel in viral replication: *i)* compound **47a**, which is active in correcting the F508del-CFTR defect and, *ii)* compound **47b**, which is inactive in correcting the F508del-CFTR defect (Figure 3). Compound **47a,b** were synthesized following the procedure reported in literature.[44]

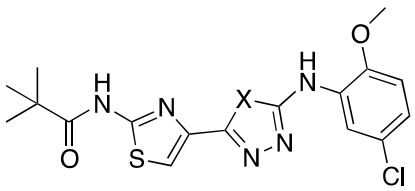

47a: X = O
47b: X = S

Figure 3. Chemical structures of compounds **47a,b**.

Biology

All the synthesized compounds were initially evaluated for their inhibitory potency against PI4KIIIβ kinase *in vitro* and for their cell-based antiviral activity: EV71 was used as the primary target for SAR exploration since compound **17** revealed the best and most reproducible antiviral activity against this virus. In particular, the antiviral activity against EV71 was evaluated in EV71-induced CPE-reduction assay in rhabdosarcoma (RD) cells. Both the EC_{50} values and the CC_{50} values were measured. Uninfected, treated cells were also inspected under the microscope to evaluate whether the compounds altered normal cell morphology. The EC_{50} and CC_{50} values allowed us to calculate the selectivity index (SI), defined as CC_{50}/EC_{50}. Compound **3** was used as a positive control. Results are summarized in Table 1.

A close correlation between the antiviral activity measured in the cell-based assay and the inhibitory potency of the PI4KIIIβ kinase was observed, with only a few exceptions. The best results were obtained via modifying the left part of the molecule. In particular compounds **25a,b**, bearing respectively a propanamide and a pivalamide moiety instead of the acetamide function of compound **17**, showed a very promising antiviral activity.

Table 1. Activity of synthesized derivatives in PI4KIIIβ inhibition assay and in virus-cell-based EV71 assay.

Compd	PI4K IIIβ IC_{50} (μM)[a]	EV71 EC_{50} (μM)	EV71 CC_{50} (μM)[b]	EV71 CC_{50} (μM)[c]	SI[d]	SI[d]
17	0.48	0.92±2.75	16.5±9.04	9.73±0.87	17.9	10.6
25a	0.27	0.38±0.10	10.1±4.82	6.37±2.46	26.6	23.6
25b	0.32	0.27±0.05	7.94±1.24	8.83±0.89	29.4	32.7
25c	21.89	2.0±0.95	25.8±5.06	30.1±9.93	12.9	15.0
25d	18.85	0.51±0.14	5.75±2.12	11.8±4.56	11.3	23.1
25e	>50	>44.6	ND[e]	ND	ND	ND
25f	>50	>55.7	ND	ND	ND	ND
25g	4.67	1.42±0.04	42.3±4.94	101.0±15.8	29.7	71.1
26a	7.69	NA[f]	ND	ND	ND	ND
26b	>50	NA	ND	ND	ND	ND
26c	1.82	2±0.04	8.87±3.85	ND	4.4	ND
26d	>50	NA	ND	ND	ND	ND
30a	3.95	4.77±0.28	20.9±6.97	ND	4.4	ND
30b	12.40	NA	ND	ND	ND	ND
35a	2.48	1.93±0.81	18.6±6.01	ND	9.64	ND
35b	2.63	NA	ND	ND	ND	ND
35c	1.55	1.2±0.16	9.17±0.85	ND	5.9	ND
35d	3.71	0.68±0.04	5.59±0.32	ND	8.2	ND
38	>50	>90.2	85.7	64.2	ND	ND
42a	NA	NA	ND	ND	ND	ND
42b	NA	NA	ND	ND	ND	ND
46	50.00	8.58±0.77	51.6±27.1	142.0±62.8	6	ND
47a	NA	NA	ND	ND	ND	ND
47b	NA	NA	ND	ND	ND	ND
3[g]	0.06	0.73	>125	-	-	-

[a]Values are the mean of at least three independent experiments. [b]CC_{50} values were assessed by MTS method. [c]CC_{50} values were determined by microscopically detectable alteration of cell morphology. [d]Selectivity index ($SI = CC_{50}/EC_{50}$). [e]ND = not determined. [f]NA = not active. [g]Reference 13

Compounds **25a,b** inhibited PI4KIIIβ and exhibited a significant antiviral effect at sub-micromolar concentrations, demonstrating a better activity than compound **17**. Compound **25g**, characterized by the Boc amino group, proved to be the most interesting compound of the entire series showing the highest selectivity index in the EV71 cell-based assay. Also changing the right portion of hit compound **17** gave interesting results (compounds **35a,c,d**). The central bithiazole scaffold proved to be essential for antiviral activity, as changing it gave inactive compounds (compounds **38**, **42a,b**). Finally, the reported compounds **46, 47a,b** were devoid of antiviral activity and PI4KIIIβ inhibition activity.

Based on these activity data, and considering that the SI of a promising antiviral candidate should be at least greater than 10, compounds **17**, **25a-d, 25g** were selected for further studies. The broad-spectrum activity of the six selected compounds was evaluated against a panel of enteroviruses representative of all major groups: enterovirus group B (coxsackievirus B3 and echovirus11, ECHO11), group C (poliovirus 1), group D (enterovirus 68), rhinovirus group A (RV02) and rhinovirus group B (RV14) (see the Experimental Section for details). Results are reported in Table 2. The selected compounds showed micromolar and sub-micromolar activity against different enteroviruses within the tested panel. In addition, the antiviral activity of the less toxic compound **25g** was confirmed against a representative panel of EV71 clinical isolates. As shown in Table 3, we could confirm the activity of compounds **25g** against the clinically relevant EV71 specimens. Only the (sub)genogroup B5 appeared to be less sensitive. Furthermore we evaluated the lipid kinase isoform selectivity of our best PI4KIIIβ inhibitors by testing them in an *in vitro* inhibition assay on the related enzyme PI4KIIIα and PI3K-α/p85α (Table 4).

Table 2. Evaluation of the broad-spectrum antiviral activity of the most potent derivatives against a representative panel of enteroviruses.

Compd	CVB3		ECHO11		PV1		EV68		RV14		RV02	
	EC_{50} (μM)	CC_{50} (μM)	EC_{50} (μM)	CC_{50} (μM)	EC_{50} (μM)	CC_{50} (μM)	EC_{50} (μM)	CC_{50} (μM)	EC_{50} (μM)	CC_{50} (μM)	EC_{50} (μM)	CC_{50} (μM)
17	2.17	101± 33.6	1.57± 0.23	>268	3.09	>269	NA[a]	ND[b]	>268	ND	NA[b]	ND
25a	2.16	89.1± 16.2	0.97	12±4. 07	<1.52	5.49± 1.42	NA	ND	NA	ND	>259	ND
25b	ND	20.9± 3.83	0.72± 0.05	5.07± 1.24	<1.41	5.07± 1.3	1.38	3.09	4.85± 1.09	ND	2.01± 0.05	ND
25c	3.87± 0.23	58.8± 7.14	3.51	29.3± 1.78	2.86± 0.36	30.3± 3.66	ND	ND	10.6± 0.7	ND	10.6± 0.2	ND
25d	2.19± 0.23	45.1± 4.44	1.77± 0.13	145±2 7.6	2.23± 0.4	145±2 7.6	NA	ND	>230	ND	2.05± 0.36	ND
25g	2.74± 0.17	80.1± 6.97	2.93	124±7 .94	13.3± 1.9	124±7 .94	ND	ND	>232	ND	ND	ND

[a]NA = not active. [b]ND = not determined

Results showed a higher specificity of the tested bithiazole derivatives for the PI4KIIIβ isoform with poor inhibition of both PI4KIIIα and PI3K-α/p85α at 100 μM concentration of each compound. The specificity of compound **25g** was also tested on a small panel of unrelated kinases: it shows only a low inhibitory effect on Src and CDK6. Despite the latter enzymes being involved in cell cycle regulation and representing common targets of antitumor compounds, **25g** did not show any toxicity or morphology alteration at antiviral concentration in the tested cell lines. In addition, recent studies indicated that Src inhibitors have no effect on EV71 replication[45] while CDK6 seems to be down-regulated in response to EV71 infection.[46] Finally, compounds reported in Table 4 were evaluated for their CFTR

Table 3. Evaluation of the antiviral activity of compound **25g** against EV71 clinical isolates.

Genogroup	Strain	Genbank	EC_{50} (μM)[a]
			Compd **25g**
B2	11316	AB575927	<1.39
B5	TW/96016/08	GQ231942	21.00
	TW/70902/08	GQ231936	3.58
C2	H08300 461#812	-	0.97
C4	TW/1956/05	GQ231926	<1.39
	TW/2429/04	GQ231927	1.17

[a]All values are based on at least three independent dose-response curves.

Table 4. Inhibitory effect of selected compounds against members of PIK family and profiling of compound **25g** against a small panel of unrelated kinases.

Compd	PI4KIIIβ	PI4KIIIα	PI3K-α/p85α	Compd	kinase	% Residual activity at 100 μM[a]
	IC_{50}(μM)[a]	% Residual activity at 100 μM[a]				
17	0.48	52	37	**25g**	Src FL	32
25a	0.27	72	40		GSK3β	79
25b	0.32	71	93		Hck FL	100
25c	21.89	73	85		FAK	82
25d	18.85	81	54		DYRK1A	88
25g	4.67	69	64		ABL FL	53
35a	2.48	58	81		FLT3	59
35c	1.55	71	51		CDK2/cA2	62
35d	3.71	73	100		CDK9/cT1	57
					CDK9/cK	49
					CDK6/cD1	25
					Pim1	70

[a]Values are the mean of two independent replicates

corrector/potentiator activity, to identify molecules that may be endowed with dual antiviral/CFTR modulator activity. As shown in Figure 4A, some of the compounds (**25a**, **25d**, **25g**) acted as CFTR correctors, increasing steady-state levels of F508del-CFTR at the plasma membrane after chronic (24 hour) incubation. Compound **48** (Lumacaftor), the leading corrector drug,[47] was used as a benchmark. This increased CFTR plasma membrane density was measured with a recently developed assay exploiting a CFTR fusion to a pH-sensitive protein.[48] The improvement in biogenesis also lead to increased anion permeability, estimated from fluorescence quenching of a CFTR-fused YFP probe following extracellular I^- addition (Figure 4B). None of the compounds acted as "potentiators" rapidly increasing anion permeability, when added only immediately prior to I^- addition (Figure 4C). The approved potentiator drug **49** (Ivacaftor) was used as a comparison.[49] Overall, the drug-induced changes in the iodide entry rate and in membrane density followed similar patterns, suggesting that the chemically corrected molecules of F508del-CFTR that reached the plasma membrane displayed an ion-channel function similar to those corrected by treatment with **48**. However, compound **25d** appears to increase CFTR membrane density more than expected from its effect on anion permeability (Figure 4D). Further studies will be required to understand the underlying mechanism. Overall, the collected biological data indicates that a fine chemical tuning of the bithiazole substituents is needed to generate compounds able to specifically inhibit the PI4KIIIβ kinase and block the replication of different enteroviruses while also correcting the F508del-CFTR folding defect. It is interesting to note that the most promising CFTR correctors (**25a**, **25d**, **25g**) are also the most active broad-spectrum antivirals and represent the first example of multi-target agents for tightly associated pulmonary diseases like enterovirus infection and cystic fibrosis.

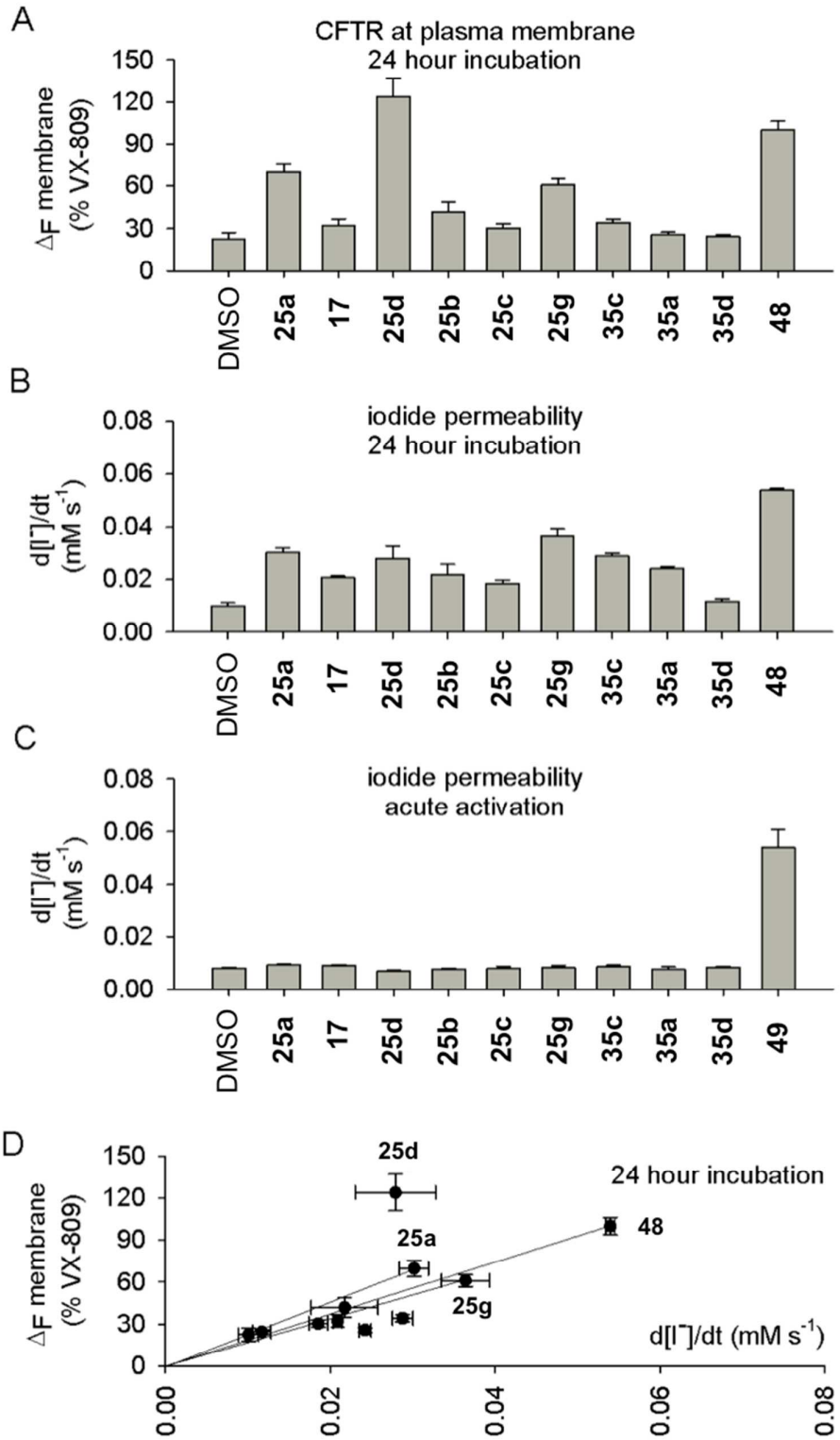

Figure 4. Effects of selected compounds on CFTR biogenesis and function. All treatments were carried out alongside low temperature incubation, known to improve F508del-CFTR membrane-localization and used to increase the fluorescence signal. A) F508del-CFTR-

pHTomato present at the plasma membrane was quantified following 24 h incubation in 10 μM of each drug. Incubation with **48** (Lumacaftor) was assessed in parallel, as a positive control. B) Anion permeability quantified using a YFP-F508del-CFTR probe following 24 h treatment as in A). C) Compounds (10 μM) do not cause an immediate change in anion permeability. Potentiator compound **49** (Ivacaftor) was used as a positive control. D) For most compounds, there is a similar ratio describing increase in membrane density over anion permeability as caused by **48** (Lumacaftor).

Molecular modelling and SAR

The hit compound **17** was docked with the Glide software[50] (SP) in the ATP binding site of the PI4KIIIβ crystal structure (PDB ID: 4D0L)[34] centering the grid on compound **1**. The predicted binding mode and interaction profile of compound **17** is very similar to that of compound **1** (Figure 5). The NH-acetamide moiety of **17** is hydrogen bonded to VAL598, which also interact with the thiazole nitrogen. The thiazole ring is involved in a Pi-Pi stacking with TYR583, while the phenyl ring is involved in a Pi-cation interaction with LYS549. The O carbonyl moiety is hydrogen bonded to LYS377. Moreover, the binding mode is completed by a series of hydrophobic interactions involving LEU383, ALA602, VAL599, VAL602, LEU663, ILE595, TYR583, ILE671, ILE673, PRO381 and LEU374. The first series of derivatives of the hit compound **17** encompasses different substitution on the left part of the molecule (right part as per Figure 5-7 representation) by replacing the methyl group of the acetamide moiety with different groups. Changing the methyl of the acetamide with an ethyl or *tert*-butyl group (**25a,b**) caused a 2-fold increase of potency, but the substitution with more hydrophobic and therefore more sterically bulky groups first reduced the potency (**25d**) and then led to a complete loss of activity (**25e**,**f**). The limit seems

to be a *tert*-butoxycarbonyl group (**25g**) which still maintains low micromolar activity (Figure 6).

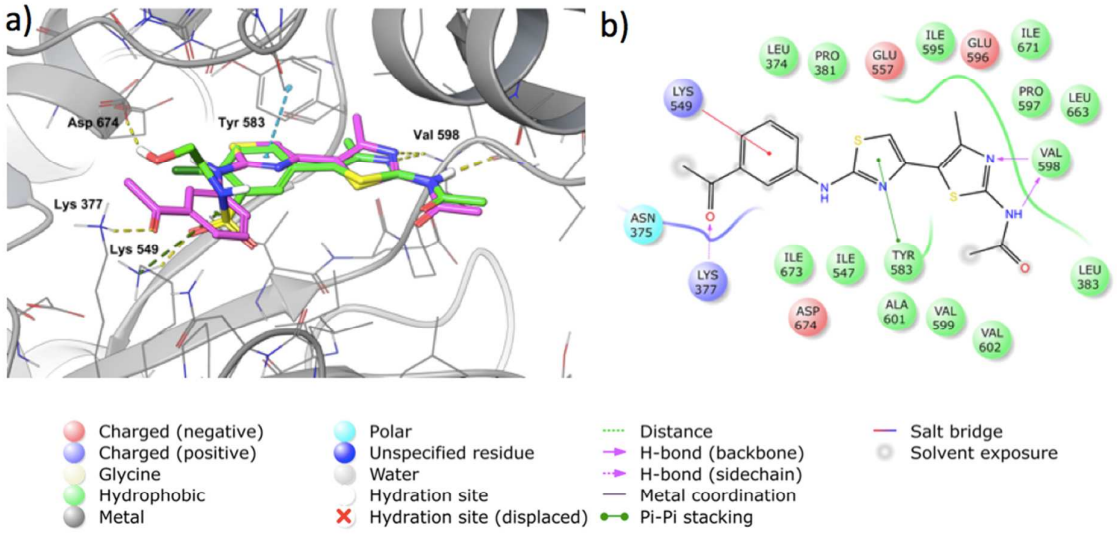

Figure 5. a) Predicted binding mode of the hit **17** (magenta sticks) superimposed to compound **1** (green sticks) into the binding site of PI4KIIIβ. b) 2D ligand interaction diagram of **17**.

The substitution of the acetamide methyl with a CF_3 (**25c**) weakened the inhibition (45-fold decrease) not due to steric reasons, but probably because of the electron withdrawing properties of the CF_3 group. Changing the acetamide moiety with a ureidic moiety caused a slight decrease in potency (**26a**,**c** and **30a**,**b**). The ureidic portion seems to interact with a double hydrogen bond to VAL598 but at the same time, the hydrophobic NH substituent moves away from the protein resulting in a solvation penalty (Figure 6). Finally, modifying a ureidic group with a thioureidic moiety caused a complete loss of activity (**26b,d**).

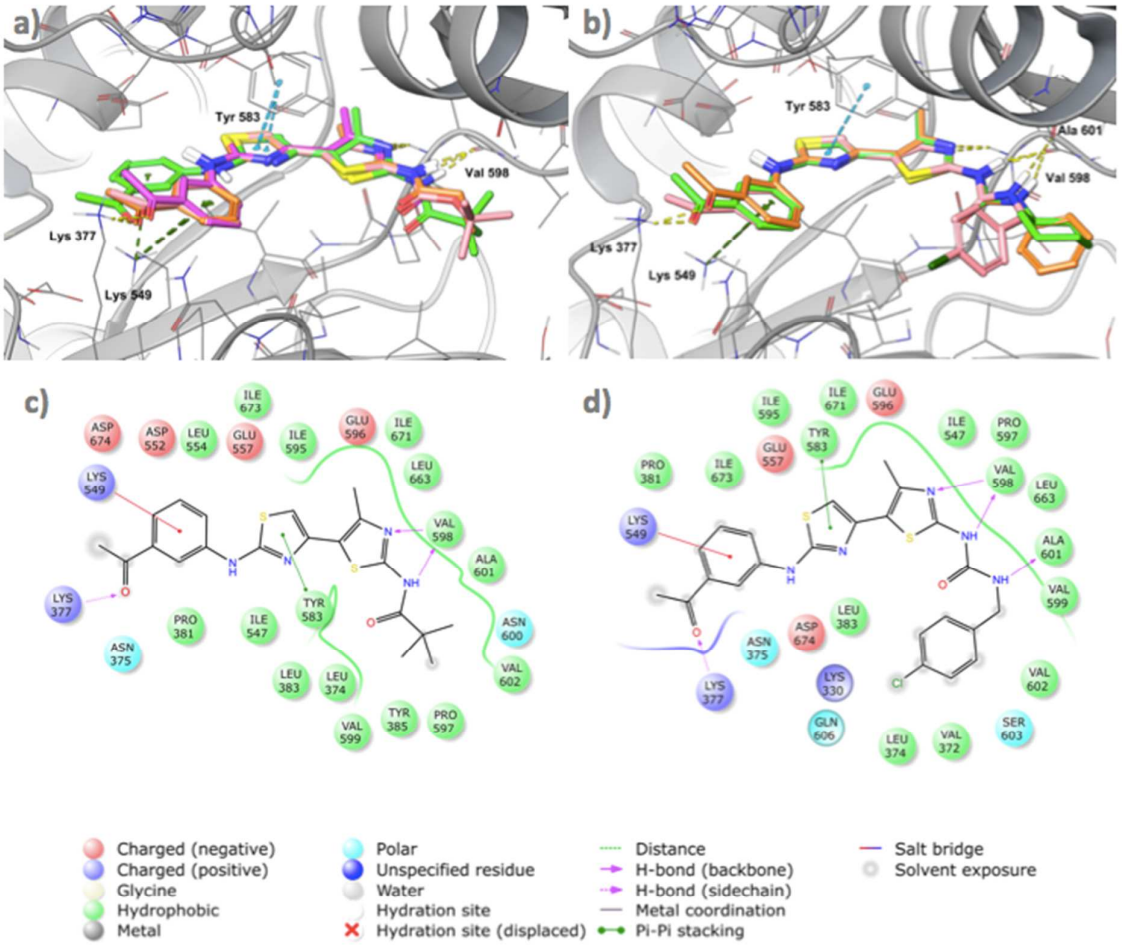

Figure 6. a) Superimposed binding modes of compounds **17** (purple sticks), **25a** (orange sticks), **25b** (green sticks) and **25g** (pink sticks) into the binding site of PI4KIIIβ. b) Superimposed binding modes of compounds **26a** (orange sticks), **26c** (green sticks) and **30a** (pink sticks) into the binding site of PI4KIIIβ. c) 2D ligand interaction diagram of **25b**. d) 2D ligand interaction diagram of **30a**.

The second series of derivatives of the hit compound **17** comprises different substitutions on the right part of the molecule (left part as per Figure 5-7 representation) by changing the substitution pattern of the phenyl ring. A change in the position of the acetyl group reduces the potency by about 10-fold (**35d**), and the same happens by introducing hydroxy and

methoxy groups in the meta position (**35b,c**). The precise positioning of the hydrogen-bond acceptor on the phenyl ring seems therefore important in improving the affinity for the enzyme. Surprisingly, the deletion of the ketonic group reduces but does not abolish activity (**35a**). The lack of the substituent on the phenyl ring deletes a hydrogen bond, but allows optimization of the other interactions, in particular the Pi-cation with lysine 549.

The last series of derivatives of the hit compound **17** encompasses modifications of the bithiazole scaffold and closely related analogues reported as DC-SIGN inhibitors and CFTR correctors. Replacement of the thiazole group of compound **17** with an imidazole (**38**) or conversion of the bithiazole scaffold into a N,N'-diarylthiourea (**42a,b**) changes the binding mode and abolishes the activity. Finally, also the DC-SIGN inhibitor **46** and CFTR correctors **47a,b** presented a suboptimal interaction profile with PI4KIIIβ and resulted in a complete loss of activity. As reported by Warrem et al.[51], docking programs and scoring functions present a few limitations in correlating subtle structural differences of active ligands with their enzymatic activity. This error is quite limited within homologous series of compounds but it can be very important for structurally unrelated compounds.[52] Our docking studies were in fact able to distinguish between active and inactive compounds but it is no coincidence that the reference compound **3**, whose scaffold is very different from those of our series, showed a docking score that is not in line with its enzymatic potency (Table 5). The most active compounds **17**, **25a** and **25b** also showed the best specificity for PI4KIIIβ over PI4KIIIα, which seems to depend on the steric hindrance of the acetamide substitution. In fact, considering compounds **17, 25a, 25b**, **25g** and **25d** that differ only for the bulkiness of the amide substituents in position C2 of the thiazole (methyl, ethyl, *tert*-butyl, *tert*-butoxy and phenyl, respectively), the affinity for PI4KIIIα decreases going from **17** to **25d** (see Table 4).

Table 5. Correlation between IC_{50} and docking score for the synthesized compounds.

Compd	PI4K IIIβ IC_{50} (μM)[a]	Docking score[b]	Compd	PI4K IIIβ IC_{50} (μM)[a]	Docking score[b]
35d	3.71	-8,297	**25e**	>50	-7,431
30b	12.40	-8,222	**26d**	>50	-7,4
26a	7.69	-8,172	**25f**	>50	-7,356
26c	1.82	-8,108	**38**	>50	-7,355
17	0.48	-8,035	**42a**	>50	-7,251
25a	0.27	-8,012	**26b**	>50	-7,144
25d	18.85	-7,983	**42b**	>50	-7,052
30a	3.95	-7,97	**25c**	21.90	-6,678
35b	2.63	-7,726	**3**[c]	0.06	-6,553
46	50.00	-7,644	**47b**	>50	-6,424
25g	4.67	-7,63	**47a**	>50	-6,148
35c	1.55	-7,605	**25e**	>50	-7,431
35a	2.48	-7,6			
25b	0.32	-7,484			

[a]Values are the mean of at least three independent experiments. [b]Docking score was calculated by the software Gold and expressed as Kcal/mol. [c]Reference 13

The higher the bulkiness in C2 of the thiazole, the lower the affinity for PI4KIIIα over PI4KIIIβ with the phenyl substituent (**25d**) representing the highest tolerated hindrance after which the inhibition of PI4KIIIβ is also compromised. The reason for the specificity of these compounds towards PI4KIIIβ seems to depend on the different opening (compared to the α isoform) of a specific loop that in the β isoform goes from ILE595 to ILE604 (Figure 7). In fact in this portion of protein, the sequence of PI4KIIIβ resembles more the sequence of PI3K (α, γ end δ) than the sequence of PI4KIIIα. In particular, the presence of a cysteine residue in position 30 of PI4KIIIα (corresponding to proline 597 in PI4KIIIβ) could change the fold of this "selectivity loop".

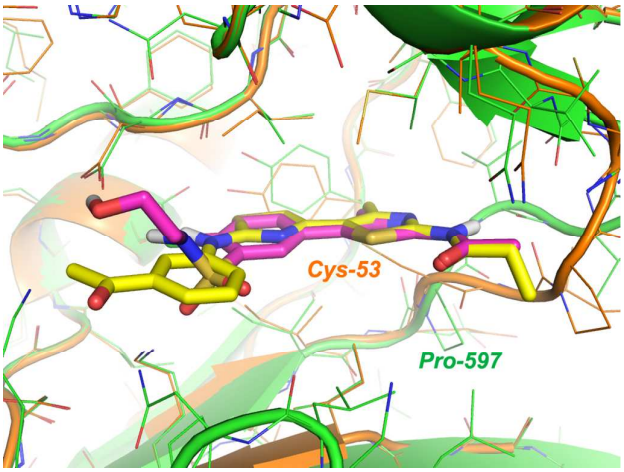

Figure 7. Observed binding mode of **25a** (yellow sticks) superimposed to compound **1** (magenta sticks) into the binding site of PI4KIIIβ (green ribbons). The orange ribbons represent the modelled structure of PI4KIIIα.

CONCLUSIONS

An increasing number of reports suggest a causal link between enterovirus infections and pulmonary exacerbations in CF patients. We report the discovery of a new class of multi-target agents active as broad-spectrum antivirals and correctors of the F508del-CFTR folding defect. To identify these drug candidates, we first carried out a virtual screening on the PI4KIIIβ (a host protein involved in enterovirus replication) catalytic site to select commercially available compounds: our choice was based on the best-predicted affinity for the target kinase and 2D similarity (in a few cases) to known CFTR correctors/potentiators. Among the selected compounds, hit **17** showed activity in cell-free PI4KIIIβ inhibition assay and cell-based enterovirus replication assays and was therefore considered a promising starting point for further structure-based optimization. A small collection of analogues of compound **17** was then designed, synthesized and biologically evaluated for their *i*) activity against panel of enteroviruses representative of all major groups; *ii*) inhibition of lipid kinases PI4KIIIβ, PI4KIIIα and PI3K-α/p85α; *iii*) corrector/potentiator activity on F508del-CFTR.

Three compounds (**25a**, **25d**, **25g**) were finally identified as novel multi-target agents able to act as broad-spectrum-antivirals (enterovirus family) and as correctors of F508del-CFTR folding defect. These compounds represent a valuable starting point to develop a novel polypharmacological approach for the treatment of closely-related pulmonary diseases such as cystic fibrosis and enterovirus infections with a single pill.

EXPERIMENTAL SECTION

Molecular modeling

Homology modeling

The structure of PI4KIIIβ was built with the Prime[53] 38013 software on the basis of the crystal structure 2CHZ using ClustalW for sequence alignment and knowledge-based as building method. The structure of PI4KIIIα was built with the online server 3D-JIGSAW[54] on the basis of the crystal structure 4D0L.

Molecular dynamics

The structure of modelled PI4KIIIβ was aligned to the 2CHZ structure. Compound **1** was extracted from 2CHZ and was manually introduced in the structure of PI4KIIIβ. A molecular dynamics simulation of the resulting complex was performed using Desmond v40013. The complex was neutralized using sodium counter ions. The complex and the counter ions were immersed in a orthorhombic periodic SPC water bath that extended about 10 Å in each direction. After an initial default relaxation protocol, a MD production run was performed for 10 ns with a time step of 2 fs.

Virtual screening

From the last 2 ns of the dynamics simulation 100 frames were extracted and clustered on the basis of RMSD. Five clusters were generated. The protein representative of each cluster was processed with the Schrödinger Suite 2014-3[55] Protein Preparation Wizard tool. On each

structure a grid was generated with the software Glide 65013 centering the grid on compound **1**, then all PI4KIIIβ ligands available from the Pubchem database were docked with the SP protocol. Structures were selected for virtual screening on the basis of their enrichment factor. The Mid Asinex database was extracted from the ZINC database[56] and docked in the binding site of compound **1** using compound **1** as the center of the grid. The software Glide 65013 with the SP protocol was used for High throughput docking. The best 1000 compounds in terms of the docking score were selected and submitted to one more docking cycle of docking with the XP protocol. On the basis of the docking score and a visual inspection 25 compounds were selected and 13 compounds were purchased.

Ligand preparation

Ligands were prepared with the LigPrep[57] tool available in the Schrödinger Suite 2015-4. Ionization states were generated at pH 7.0 ± 2.0 with Epik.

Ligand docking

The X-ray coordinates of PI4KIIIβ in complex with compound **1** were extracted from the Protein Data Bank (PDB code 4D0L). The structure was then processed with the Schrödinger Suite 2015-4 Protein Preparation Wizard tool.[58] The A Chain was selected, water molecules were removed, and an exhaustive sampling of the orientations of groups, whose hydrogen bonding network needs to be optimized, was performed. Finally, the protein structure was refined to relieve steric clashes with a restrained minimization with the OPLS3 force field[59] until a final RMSD of 0.30 Å with respect to the input protein coordinates.

Docking studies were performed using Glide[60] 69017 with the SP protocol. The protein structure, prepared as described above, was used to build the energy grid. The enclosing box was centered on the cocrystallized ligand. All parameters were set to their default value. The docking protocol was validated by redocking the cocrystallized ligand (compound **1)**.

Chemistry

General. All commercially available chemicals were purchased from both Sigma- Aldrich and Alfa Aesar and, unless otherwise noted, used without any previous purification. Solvents used for work-up and purification procedures were of technical grade. Dry solvents used in the reactions were obtained by distillation of technical grade materials over appropriate dehydrating agents. Reactions were monitored by thin layer chromatography on silica gel-coated aluminium foils (silica gel on Al foils, SUPELCO Analytical, Sigma-Aldrich) at 254 and 365 nm. Where indicated, products were purified by silica gel flash chromatography on columns packed with Merck Geduran Si 60 (40-63 μm). ^{1}H and ^{13}C NMR spectra were recorded on BRUKER AVANCE 300 MHz and BRUKER AVANCE 400 MHz spectrometers. Chemical shifts (δ scale) are reported in parts per million relative to TMS. ^{1}H-NMR spectra are reported in this order: multiplicity and number of protons; signals were characterized as: *s* (singlet), *d* (doublet), *t* (triplet), *q* (quadruplet), *m* (multiplet), *bs* (broad signal). ESI-mass spectra were recorded on an API 150EX apparatus and are reported in the form of (m/z). Elemental analyses were performed on a Perkin-Elmer PE 2004 elemental analyzer. Melting points were taken using a Gallenkamp melting point apparatus and were uncorrected. All final compounds showed chemical purity ≥95% as determined by elemental analysis data for C, H, and N (within 0.4% of the theoretical values).

*Synthesis of N-(2-((3-acetylphenyl)amino)-4'-methyl-[4,5'-bithiazol]-2'-yl)acetamide (**17**).* Et_3N (84 μL, 0.60 mmol) was added to a stirred suspension of intermediate **24** (100 mg, 0.30 mmol) in dry DCM (4 mL) at 0 °C. After 15 minutes acetyl chloride (32 μL, 0.45 mmol), diluted in dry DCM (0.5 mL), was added dropwise. The resulting solution was warmed to room temperature and stirred for 15 h. Next, H_2O and DCM were added and the aqueous phase was extracted twice with DCM. The combined organic phases were washed with brine,

dried over Na_2SO_4 and evaporated. The crude was purified by flash chromatography using DCM/MeOH (98/2) as eluent to afford compound **17** as a yellow solid. Yield 77%; mp 244-246 °C. MS (ESI) $[M + H]^+$: 373.3 *m/z*. ^{1}H NMR (DMSO-d_6 300 MHz): δ 2.14 (s, 3H), 2.51 (s, 3H), 2.63 (s, 3H), 6.95 (s, 1H), 7.48 (t, 1H, J = 7.9 Hz), 7.56 (d, 1H, J = 7.9 Hz), 7.77 (d, 1H, J = 7.9 Hz), 8.51 (s, 1H), 10.56 (s, 1H), 12.06 (s, 1H). ^{13}C NMR (DMSO-d_6 100.6 MHz): δ 17.56, 22.92, 27.42, 103.25, 116.75, 120.52, 121.44, 121.65, 129.79, 138.11, 141.81, 143.21, 143.29, 155.58, 162.92, 168.73, 198.28. Anal. ($C_{17}H_{16}N_4O_2S_2$) C, H, N.

*Synthesis of 1-(2-amino-4-methylthiazol-5-yl)ethanone (**20**).* A solution of thiourea **18** (283 mg, 3.72 mmol) and 3-chloro-2,4-pentanedione **19** (419 µL, 3.72 mmol) in ethanol (20 mL) was heated at reflux for 12 h, and then the reaction mixture was cooled down to 0 °C. The precipitate was separated by filtration over a Buchner funnel and washed with cold ethanol and ether to afford the product **20** as a white solid. Yield 95%. MS (ESI) $[M + H]^+$: 157.2 *m/z*. ^{1}H NMR (DMSO-d_6 400 MHz): δ 2.44 (s, 3H), 2.52 (s, 3H), 9.49 (bs, 2H).

*Synthesis of 1-(2-amino-4-methylthiazol-5-yl)-2-bromoethanone (**21**).* A suspension of intermediate **20** (500 mg, 3.20 mmol) in 48% HBr solution in water (10 mL) was warmed to 60 °C. A solution of Br_2 (148 µL, 2.88 mmol) in 1,4-dioxane (10 mL) was added dropwise and the reaction mixture was heated at 60 °C for 3 h. After cooling down to room temperature, saturated aqueous $NaHCO_3$ solution and ethyl acetate were added and the aqueous phase was extracted three times with ethyl acetate. The combined organic phases were washed with brine, dried over Na_2SO_4 and concentrated under vacuum to obtain compound **21**, used in the next step without any further purification. Yield 90%. MS (ESI) $[M + H]^+$: 235.0 *m/z*, $[M + 2 + H]^+$: 237.1 *m/z*. ^{1}H NMR (DMSO-d_6 400 MHz): δ 2.46 (s, 3H), 4.48 (s, 2H), 9.18 (bs, 2H).

*Synthesis of 1-(3-acetylphenyl)thiourea (**23**).* Benzoyl isothiocyanate (547 µL, 4.07 mmol) was added dropwise to a solution of 3'-aminoacetophenone **22** (500 mg, 3.70 mmol) in dry

DCM (12 mL) and the mixture was stirred at room temperature for 12 h. The solvent of reaction was evaporated, the residue was dissolved in THF/NaOH 1N (1/1, 15 mL) and the mixture was refluxed for 3 h. After cooling to room temperature, H_2O and ethyl acetate were added and the aqueous phase was extracted twice with ethyl acetate. The combined organic phases were dried over Na_2SO_4 and evaporated. The resulting solid was crystallized from ether. Yield 72%. MS (ESI) $[M + H]^+$: 195.1 *m/z*. ^{1}H NMR (DMSO-d_6 400 MHz): δ 2.57 (s, 3H), 7.46 (t, 1H, J = 7.9 Hz), 7.55 (bs, 2H), 7.70-7.73 (m, 2H), 8.03 (s, 1H), 9.89 (s, 1H).

*Synthesis of 1-(3-((2'-amino-4'-methyl-[4,5'-bithiazol]-2-yl)amino)phenyl)ethanone (**24**).* Intermediates **21** (200 mg, 0.85 mmol) and **23** (165 mg, 0.85 mmol) were suspended in ethanol (5 mL) and the mixture was heated at reflux for 1 h. Then saturated aqueous $NaHCO_3$ solution and ethyl acetate were added to the mixture and the aqueous phase was extracted three times with ethyl acetate. The combined organic phases were washed with brine, dried over Na_2SO_4 and concentrated under vacuum. Ether was added to the crude and the solid obtained was filtered over a Buchner funnel, washed with ether and used in the following step without any further purification. Yield 84%. MS (ESI) $[M + H]^+$: 331.3 *m/z*. ^{1}H NMR (DMSO-d_6 300 MHz): δ 2.35 (s, 3H), 2.60 (s, 3H), 6.67 (s, 1H), 7.09 (bs, 2H), 7.46 (t, 1H, J = 7.9 Hz), 7.55 (d, 1H, J = 7.9 Hz), 7.75 (d, 1H, J = 7.9 Hz), 8.40 (s, 1H), 10.55 (s, 1H).

*General Procedure for the Synthesis of Compounds **25a-g**.*

*Method A (for **25a-c**).* Et_3N (84 µL, 0.60 mmol) was added to a stirred suspension of intermediate **24** (100 mg, 0.30 mmol) in dry DCM (4 mL) at 0 °C. After 15 minutes the proper acyl chlorides or anhydride (0.45 mmol), diluted in dry DCM (0.5 mL), were added dropwise. The resulting solution was warmed to room temperature and stirred for 12-15 h. Next, H_2O and DCM were added and the aqueous phase was extracted twice with DCM. The combined organic phases were washed with brine, dried over Na_2SO_4 and evaporated. The crude was purified by flash chromatography using DCM/MeOH (98/2) as eluent.

*N-(2-((3-acetylphenyl)amino)-4'-methyl-[4,5'-bithiazol]-2'-yl)propionamide (**25a**).* Yield 75%; mp 244-246 °C. MS (ESI) $[M + H]^+$: 387.1 *m/z*. ^{1}H NMR (DMSO-d_6 400 MHz): δ 1.11 (t, 3H, J = 7.5 Hz), 2.45 (q, 2H, J = 7.5 Hz), 2.52 (s, 3H), 2.64 (s, 3H), 6.95 (s, 1H), 7.50 (t, 1H, J = 7.9 Hz), 7.57 (d, 1H, J = 7.9 Hz), 7.82 (d, 1H, J = 7.9 Hz), 8.47 (s, 1H), 10.56 (s, 1H), 12.03 (s, 1H). ^{13}C NMR (DMSO-d_6 100.6 MHz): δ 9.63, 17.56, 27.43, 28.69, 103.25, 116.72, 120.47, 121.49, 121.63, 129.82, 138.11, 141.82, 143.24, 143.33, 155.62, 162.94, 172.36, 198.28. Anal. ($C_{18}H_{18}N_4O_2S_2$) C, H, N.

*N-(2-((3-acetylphenyl)amino)-4'-methyl-[4,5'-bithiazol]-2'-yl)pivalamide (**25b**).* Yield 80%; mp 232-234 °C. MS (ESI) $[M + H]^+$: 415.4 *m/z*. ^{1}H NMR (DMSO-d_6 400 MHz): δ 1.25 (s, 9H), 2.53 (s, 3H), 2.63 (s, 3H), 6.95 (s, 1H), 7.50 (t, 1H, J = 7.9 Hz), 7.57 (d, 1H, J = 7.9 Hz), 7.85 (d, 1H, J = 7.9 Hz), 8.43 (s, 1H), 10.57 (s, 1H), 11.79 (s, 1H). ^{13}C NMR (DMSO-d_6 100.6 MHz): δ 16.45, 26.90, 27.05 (3x), 39.24, 102.80, 117.29, 120.96, 122.25, 122.46, 129.67, 138.02, 140.79, 142.33, 143.58, 156.98, 163.28, 176.67, 198.36. Anal. ($C_{20}H_{22}N_4O_2S_2$) C, H, N.

*N-(2-((3-acetylphenyl)amino)-4'-methyl-[4,5'-bithiazol]-2'-yl)-2,2,2-trifluoroacetamide (**25c**).* Yield 65%; mp 254-256 °C. MS (ESI) $[M + H]^+$: 427.1 *m/z*. ^{1}H NMR (DMSO-d_6 400 MHz): δ 2.54 (s, 3H), 2.63 (s, 3H), 7.14 (s, 1H), 7.50 (t, 1H, J = 7.9 Hz), 7.58 (d, 1H, J = 7.9 Hz), 7.75 (d, 1H, J = 7.9 Hz), 8.47 (s, 1H), 10.64 (s, 1H), 14.05 (s, 1H). ^{13}C NMR (DMSO-d_6 100.6 MHz): δ 15.84, 27.41, 105.27, 115.80, 116.68, 120.50, 121.44, 121.79, 129.86, 138.12, 141.59, 143.31, 143.48, 155.43, 163.45, 168.73, 198.21. Anal. ($C_{17}H_{13}F_3N_4O_2S_2$) C, H, N.

*Method B (for **25d-f**).* Et_3N (84 µL, 0.60 mmol) was added to a stirred suspension of intermediate **24** (100 mg, 0.30 mmol) in dry DCM (4 mL) at 0 °C. After 15 minutes the proper acyl chlorides (0.45 mmol), diluted in dry DCM (0.5 mL), were added dropwise. The resulting solution was warmed to room temperature and heated at reflux for 15 h. Next, H_2O and DCM were added and the aqueous phase was extracted twice with DCM. The combined

organic phases were washed with brine, dried over Na_2SO_4 and evaporated. The crude was purified by flash chromatography using DCM/MeOH (99/1) as eluent.

N-(2-((3-acetylphenyl)amino)-4'-methyl-[4,5'-bithiazol]-2'-yl)benzamide (***25d***). Yield 75%; mp 199-200 °C. MS (ESI) $[M + H]^+$: 435.3 *m/z*. ^{1}H NMR (DMSO-d_6 400 MHz): δ 2.58 (s, 3H), 2.66 (s, 3H), 7.02 (s, 1H), 7.49-7.66 (m, 5H), 7.83 (d, 1H, J = 7.9 Hz), 8.12 (d, 2H, J = 7.8 Hz), 8.50 (s, 1H), 10.59 (s, 1H), 12.62 (s, 1H). ^{13}C NMR (DMSO-d_6 100.6 MHz): δ 17.42, 27.44, 103.60, 116.76, 121.52, 121.66, 128.61, 129.02, 129.06 (2x), 129.83 (2x), 132.59, 133.31, 138.12, 141.82, 143.23, 143.29, 155.72, 163.02, 167.79, 198.30. Anal. ($C_{22}H_{18}N_4O_2S_2$) C, H, N.

N-(2-((3-acetylphenyl)amino)-4'-methyl-[4,5'-bithiazol]-2'-yl)-4-iodobenzamide (***25e***). Yield 65%; mp 220-223 °C. MS (ESI) $[M + H]^+$: 561.3 *m/z*. ^{1}H NMR (DMSO-d_6 400 MHz): δ 2.58 (s, 3H), 2.66 (s, 3H), 7.01 (s, 1H), 7.50 (t, 1H, J = 7.9 Hz), 7.58 (d, 1H, J = 7.9 Hz), 7.81 (d, 1H, J = 7.9 Hz), 7.88 (d, 2H, J = 8.5 Hz), 7.94 (d, 2H, J = 8.5 Hz), 8.50 (s, 1H), 10.58 (s, 1H), 12.70 (s, 1H). ^{13}C NMR (DMSO-d_6 100.6 MHz): δ 17.33, 27.45, 101.14, 103.65, 116.77, 121.03, 121.51, 121.67, 129.82, 130.44 (2x), 132.34, 137.95 (2x), 138.12, 141.81, 143.16, 143.29, 154.99, 163.02, 165.15, 198.30. Anal. ($C_{22}H_{17}IN_4O_2S_2$) C, H, N.

N-(2-((3-acetylphenyl)amino)-4'-methyl-[4,5'-bithiazol]-2'-yl)-4-methylbenzamide (***25f***). Yield 72%; mp 243-244 °C. MS (ESI) $[M + H]^+$: 449.2 *m/z*. ^{1}H NMR (DMSO-d_6 400 MHz): δ 2.40 (s, 3H), 2.58 (s, 3H), 2.66 (s, 3H), 7.01 (s, 1H), 7.36 (d, 2H, J = 8.0 Hz), 7.50 (t, 1H, J = 7.9 Hz), 7.57 (d, 1H, J = 7.9 Hz), 7.82 (d, 1H, J = 7.9 Hz), 8.02 (d, 2H, J = 8.0 Hz), 8.50 (s, 1H), 10.58 (s, 1H), 12.55 (s, 1H). ^{13}C NMR (DMSO-d_6 100.6 MHz): δ 17.76, 21.55, 27.44, 103.55, 116.75, 120.52, 121.51, 121.66, 128.63 (2x), 129.62 (2x), 129.83, 131.51, 138.13, 141.42, 141.83, 143.26, 143.39, 155.78, 163.00, 168.09, 198.31. Anal. ($C_{23}H_{20}N_4O_2S_2$) C, H, N.

*Method C (for **25g**).* Et_3N (84 μL, 0.60 mmol) was added to a stirred suspension of intermediate **24** (100 mg, 0.30 mmol) in dry DMF (4 mL) at 0 °C. After 15 minutes Boc anhydride (0.60 mmol), diluted in dry DMF (0.5 mL), was added dropwise under vigorous stirring. The resulting solution was warmed to room temperature and heated at 50 °C for 12 h. Next, H_2O and ethyl acetate were added and the aqueous phase was extracted twice with ethyl acetate. The combined organic phases were washed with brine, dried over Na_2SO_4 and evaporated. The crude was purified by flash chromatography using DCM/MeOH (98/2) as eluent.

*Tert-butyl (2-((3-acetylphenyl)amino)-4'-methyl-[4,5'-bithiazol]-2'-yl)carbamate (**25g**).* Yield 63%; mp 235-236 °C. MS (ESI) $[M + H]^+$: 431.5 *m/z*. ^{1}H NMR (DMSO-d_6 400 MHz): δ 1.50 (s, 9H), 2.47 (s, 3H), 2.63 (s, 3H), 6.92 (s, 1H), 7.49 (t, 1H, J = 7.9 Hz), 7.56 (d, 1H, J = 7.9 Hz), 7.80 (d, 1H, J = 7.9 Hz), 8.50 (s, 1H), 10.54 (s, 1H), 11.39 (s, 1H). ^{13}C NMR (DMSO-d_6 100.6 MHz): δ 17.51, 27.42, 28.37 (3x), 79.61, 103.15, 116.70, 120.03, 121.24, 121.65, 128.34, 138.55, 141.83, 143.41, 143.62, 155.67, 157.03, 168.39, 198.32. Anal. ($C_{20}H_{22}N_4O_3S_2$) C, H, N.

*General Procedure for the Synthesis of Compounds **26a-d**.* A solution of intermediate **24** (100 mg, 0.30 mmol) and the proper isocyanate or isothiocyanate (0.45 mmol) in pyridine (2 mL) was heated at reflux for 12-18 h. The mixture was cooled to room temperature and diluted with ethyl acetate. The organic phase was washed with saturated aqueous NH_4Cl solution and brine, dried over Na_2SO_4, and concentrated under vacuum. The crude was purified by flash chromatography using DCM/MeOH (98/2) as eluent.

*1-(2-((3-acetylphenyl)amino)-4'-methyl-[4,5'-bithiazol]-2'-yl)-3-phenylurea (**26a**).* Yield 59%; mp 236-239 °C. MS (ESI) $[M + H]^+$: 450.3 *m/z*. ^{1}H NMR (DMSO-d_6 400 MHz): δ 2.51 (s, 3H), 2.64 (s, 3H), 6.92 (s, 1H), 7.05 (t, 1H, J = 7.4 Hz), 7.33 (t, 2H, J = 7.4 Hz), 7.48-7.52 (m, 3H), 7.57 (d, 1H, J = 7.8 Hz), 7.80 (d, 1H, J = 7.8 Hz), 8.47 (s, 1H), 8.99 (s, 1H), 10.52

(s, 1H), 10.55 (s, 1H). ^{13}C NMR (DMSO-d_6 100.6 MHz): δ 17.29, 27.43, 102.86, 116.73, 119.02 (2x), 121.46, 121.62, 123.17, 128.20, 129.39 (2x), 129.83, 138.10, 139.17, 139.43, 141.83, 143.36, 151.90, 155.68, 162.92, 198.35. Anal. ($C_{22}H_{19}N_5O_2S_2$) C, H, N.

1-(2-((3-acetylphenyl)amino)-4'-methyl-[4,5'-bithiazol]-2'-yl)-3-phenylthiourea ***(26b)***. Yield 65%; mp 217-218 °C. MS (ESI) $[M + H]^+$: 466.4 *m/z*. ^{1}H NMR (DMSO-d_6 400 MHz): δ 2.54 (s, 3H), 2.64 (s, 3H), 6.99 (s, 1H), 7.07 (t, 1H, J = 7.4 Hz), 7.32 (t, 2H, J = 7.4 Hz), 7.48 (t, 1H, J = 7.8 Hz), 7.57 (d, 1H, J = 7.8 Hz), 7.69 (d, 1H, J = 7.8 Hz), 7.73 (d, 2H, J = 7.4 Hz), 8.57 (s, 1H), 10.20 (s, 1H), 10.59 (s, 1H), 12.68 (s, 1H). ^{13}C NMR (DMSO-d_6 100.6 MHz): δ 17.30, 27.60, 103.92, 116.74, 121.50, 121.77, 122.48, 127.80, 128.20 (2x), 128.84 (2x), 129.81, 138.12, 138.30, 139.89, 141.73, 142.96, 155.60, 163.20, 176.12, 198.28. Anal. ($C_{22}H_{19}N_5OS_3$) C, H, N.

1-(2-((3-acetylphenyl)amino)-4'-methyl-[4,5'-bithiazol]-2'-yl)-3-cyclohexylurea ***(26c)***. Yield 69%; mp 197-198 °C. MS (ESI) $[M + H]^+$: 456.4 *m/z*. ^{1}H NMR (DMSO-d_6 400 MHz): δ 1.14-1.38 (m, 6H), 1.52-1.56 (m, 1H), 1.64-1.68 (m, 2H), 1.80-1.83 (m, 2H), 2.45 (s, 3H), 2.61 (s, 3H), 6.53 (d, 1H, J = 7.8 Hz), 6.84 (s, 1H), 7.48 (t, 1H, J = 7.8 Hz), 7.56 (d, 1H, J = 7.8 Hz), 7.85 (d, 1H, J = 7.8 Hz), 8.41 (s, 1H), 10.09 (s, 1H), 10.52 (s, 1H). ^{13}C NMR (DMSO-d_6 100.6 MHz): δ 17.53, 24.67, 25.58, 27.41 (2x), 33.12 (2x), 48.44, 102.47, 116.67, 120.57, 121.45, 121.57, 129.81, 138.07, 141.85, 143.61, 147.01, 155.38, 157.13, 162.82, 198.29. Anal. ($C_{22}H_{25}N_5O_2S_2$) C, H, N.

1-(2-((3-acetylphenyl)amino)-4'-methyl-[4,5'-bithiazol]-2'-yl)-3-cyclohexylthiourea ***(26d)***. Yield 52%; mp 234-236 °C. MS (ESI) $[M + H]^+$: 472.3 *m/z*. ^{1}H NMR (DMSO-d_6 400 MHz): δ 1.24-1.37 (m, 6H), 1.52-1.56 (m, 1H), 1.63-1.67 (m, 2H), 1.85-1.93 (m, 2H), 2.49 (s, 3H), 2.63 (s, 3H), 6.96 (s, 1H), 7.47 (t, 1H, J = 7.8 Hz), 7.56 (d, 1H, J = 7.8 Hz), 7.85 (d, 1H, J = 7.8 Hz), 8.41 (s, 1H), 9.55 (s, 1H), 10.57 (s, 1H), 11.41 (s, 1H). ^{13}C NMR (DMSO-d_6 100.6 MHz): δ 17.84, 24.38, 25.56, 27.50 (2x), 31.80 (2x), 52.62, 103.47, 116.67, 121.45, 121.58,

121.74, 129.79, 137.20, 138.11, 141.65, 142.93, 146.01, 163.00, 171.90, 198.11. Anal. ($C_{22}H_{25}N_5OS_3$) C, H, N.

*Synthesis of phenyl (5-acetyl-4-methylthiazol-2-yl)carbamate (**27**).* 1-(2-amino-4-methylthiazol-5-yl)ethanone **20** (1000 mg, 6.40 mmol) was added to a suspension of NaH 60% dispersion in mineral oil (768 mg, 19.20 mmol) in DMF (15 mL) at 0 °C. Diphenyl carbonate (3428 mg, 16.0 mmol) was added while cooling and the reaction mixture was stirred for additional 30 minutes at room temperature. H_2O and ethyl acetate were added and the aqueous phase was extracted three times with ethyl acetate. The combined organic phases were washed twice with an aqueous solution of LiCl (5% w/w) and brine, dried over Na_2SO_4 and concentrated under vacuum. Ether was added to the crude and the white solid obtained was filtered over a Buchner funnel, washed with ether and used in the following step without any further purification. Yield: 67%. MS (ESI) $[M + H]^+$: 277.2 *m/z*. ^{1}H NMR (DMSO-d_6 400 MHz): δ 2.52 (s, 3H), 2.57 (s, 3H), 7.27-7.34 (m, 3H), 7.44-7.48 (m, 2H), 12.71 (s, 1H).

*General Procedure for the Synthesis of Compounds **28a,b**.* The proper amine (1.09 mmol) was added to a solution of intermediate **27** (300 mg, 1.09 mmol) in dry THF (15 mL). The mixture was heated at 50 °C for 5-6 h, after which H_2O and ethyl acetate were added and the reaction mixture was cooled down to room temperature. The aqueous phase was extracted twice with ethyl acetate, the combined organic phases were washed with brine, dried over Na_2SO_4 and concentrated under vacuum. The crude was purified by flash chromatography using DCM/MeOH (97/3) as eluent.

*1-(5-acetyl-4-methylthiazol-2-yl)-3-(4-chlorobenzyl)urea (**28a**).* Yield: 61%. MS (ESI) $[M + H]^+$: 324.2 *m/z*. ^{1}H NMR (DMSO-d_6 300 MHz): δ 2.49 (s, 3H), 2.62 (s, 3H), 4.34 (d, 2H, J = 5.7 Hz), 7.18 (bs, 1H), 7.33 (d, 2H, J = 8.2 Hz), 7.40 (d, 2H, J = 8.2 Hz), 11.02 (s, 1H).

*1-(5-acetyl-4-methylthiazol-2-yl)-3-(adamantan-1-yl)urea (**28b**).* Yield: 93%. MS (ESI) [M + H]$^+$: 334.5 *m/z*. ^{1}H NMR (DMSO-d_6 300 MHz): δ 1.64-1.65 (m, 6H), 1.93-1.95 (m, 6H), 2.05-2.06 (m, 3H), 2.49 (s, 3H), 2.63 (s, 3H), 6.42 (s, 1H), 10.21 (s, 1H).

*General Procedure for the Synthesis of Compounds **29a,b**.* A suspension of the proper intermediate **28a,b (**0.62 mmol) in 48% HBr solution in water (2 mL) was warmed to 60 °C. A solution of Br_2 (42 µL, 0.81 mmol) in 1,4-dioxane (2 mL) was added dropwise and the reaction mixture was heated at 60 °C for 3 h. After cooling down to room temperature, saturated aqueous $NaHCO_3$ solution and ethyl acetate were added and the aqueous phase was extracted three times with ethyl acetate. The combined organic phases were washed with brine, dried over Na_2SO_4 and concentrated under vacuum. Intermediates **29a,b** were used in the next step without any further purification.

*1-(5-(2-bromoacetyl)-4-methylthiazol-2-yl)-3-(4-chlorobenzyl)urea (**29a**).* Yield: 88%. MS (ESI) [M + H]$^+$: 402.4 *m/z,* [M + 2 + H]$^+$: 404.3 *m/z,* [M + 4 + H]$^+$: 406.3 *m/z*. ^{1}H NMR (DMSO-d_6 300 MHz): δ 2.49 (s, 3H), 4.34 (d, 2H, J = 5.7 Hz), 4.46 (bs, 2H), 7.18 (bs, 1H), 7.36 (d, 2H, J = 8.2 Hz), 7.43 (d, 2H, J = 8.2 Hz), 11.23 (s, 1H).

*1-(adamantan-1-yl)-3-(5-(2-bromoacetyl)-4-methylthiazol-2-yl)urea (**29b**).* Yield: 92%. MS (ESI) [M + H]$^+$: 412.3 *m/z,* [M + 2 + H]$^+$: 414.3 *m/z*. ^{1}H NMR (DMSO-d_6 300 MHz): δ 1.65-1.67 (m, 6H), 1.93-1.95 (m, 6H), 2.06-2.08 (m, 3H), 2.49 (s, 3H), 4.49 (bs, 2H), 6.43 (s, 1H), 10.31 (s, 1H).

*General Procedure for the Synthesis of Compounds **30a,b**.* A suspension of intermediate **23** (100 mg, 0.51 mmol) and the proper compound **29a,b** (0.51 mmol) in ethanol (6 mL) was heated at reflux for 1 h. After cooling down to room temperature, saturated aqueous $NaHCO_3$ solution, H_2O and ethyl acetate were added and the aqueous phase was extracted three times with ethyl acetate. The combined organic phases were washed with brine, dried over Na_2SO_4

and concentrated under vacuum. The crude was purified by flash chromatography using DCM/MeOH (97/3) as eluent.

1-(2-((3-acetylphenyl)amino)-4'-methyl-[4,5'-bithiazol]-2'-yl)-3-(4-chlorobenzyl)urea ***(30a)***. Yield 78%; mp 240-241 °C. MS (ESI) $[M + H]^+$: 498.2 *m/z*. ^{1}H NMR (DMSO-d_6 400 MHz): δ 2.47 (s, 3H), 2.61 (s, 3H), 4.34 (d, 2H, J = 5.7 Hz), 6.86 (s, 1H), 7.09 (bs, 1H), 7.33 (d, 2H, J = 8.2 Hz), 7.40 (d, 2H, J = 8.2 Hz), 7.48 (t, 1H, J = 7.8 Hz), 7.55 (d, 1H, J = 7.8 Hz), 7.83 (d, 1H, J = 7.8 Hz), 8.42 (s, 1H), 10.51 (s, 1H), 10.53 (s, 1H). ^{13}C NMR (DMSO-d_6 100.6 MHz): δ 17.50, 27.41, 42.73, 102.57, 116.67, 120.01, 121.45, 121.58, 128.78 (2x), 129.54 (2x), 129.82, 131.89, 138.08, 139.25, 141.84, 143.21, 143.55, 154.41, 157.67, 162.84, 198.30. Anal. ($C_{23}H_{20}ClN_5O_2S_2$) C, H, N.

1-(2-((3-acetylphenyl)amino)-4'-methyl-[4,5'-bithiazol]-2'-yl)-3-(adamantan-1-yl)urea ***(30b)***. Yield 83%; mp 227-230 °C. MS (ESI) $[M + H]^+$: 508.5 *m/z*. ^{1}H NMR (DMSO-d_6 400 MHz): δ 1.65-1.67 (m, 6H), 1.93-1.95 (m, 6H), 2.05-2.06 (m, 3H), 2.49 (s, 3H), 2.63 (s, 3H), 6.78 (s, 1H), 6.97 (s, 1H), 7.49 (t, 1H, J = 7.8 Hz), 7.56 (d, 1H, J = 7.8 Hz), 7.81 (d, 1H, J = 7.8 Hz), 8.46 (s, 1H), 10.21 (bs, 1H), 10.59 (s, 1H). ^{13}C NMR (DMSO-d_6 100.6 MHz): δ 16.39, 27.47, 29.29 (3x), 36.32 (3x), 41.73 (3x), 51.16, 103.55, 116.76, 119.09, 121.49, 121.63, 129.83, 138.08, 139.61, 141.76, 142.58, 152.13, 158.27, 163.05, 198.32. Anal. ($C_{26}H_{29}N_5O_2S_2$) C, H, N.

*Synthesis of N-(5-acetyl-4-methylthiazol-2-yl)acetamide (**31**).* Intermediate **20** (1000 mg, 6.40 mmol) was suspended in THF/DCM (3/2, 12 mL) and the mixture was cooled down to 0 °C. Pyridine (1.3 mL) was added, followed by the dropwise addition of acetyl chloride (683 µL, 9.60 mmol). The reaction mixture was stirred at 0 °C for 3 h. Next, H_2O and ethyl acetate were added and the aqueous phase was extracted three times with ethyl acetate. The combined organic phases were washed three times with saturated aqueous NH_4Cl solution and brine, dried over Na_2SO_4 and concentrated under vacuum. Intermediate **31** was used in

the next step without any further purification. Yield: 87%. MS (ESI) $[M + H]^+$: 199.3 *m/z*. ^1H NMR (DMSO-d_6 400 MHz): δ 2.17 (s, 3H), 2.46 (s, 3H), 2.56 (s, 3H), 12.44 (s, 1H).

*Synthesis of N-(5-(2-bromoacetyl)-4-methylthiazol-2-yl)acetamide (**32**).* A solution of Br_2 (388 µL, 7.6 mmol) in 1,4-dioxane (8.6 mL) was added dropwise to a stirred solution of intermediate **31** (1200 mg, 6.05 mmol) in 1,4-dioxane (23 mL). The mixture was heated at 50 °C for 22 h. After cooling down to room temperature, saturated aqueous $NaHCO_3$ solution and ethyl acetate were added and the aqueous phase was extracted three times with ethyl acetate. The combined organic phases were washed with brine, dried over Na_2SO_4 and concentrated under vacuum. The crude was purified by flash chromatography using DCM/acetone (95/5) as eluent. Yield 84%. MS (ESI) $[M + H]^+$: 277.3 *m/z,* $[M + 2 + H]^+$: 279.4 *m/z*. ^1H NMR (DMSO-d_6 400 MHz): δ 2.11 (s, 3H), 2.46 (s, 3H), 4.52 (bs, 2H), 12.44 (s, 1H).

*General Procedure for the Synthesis of Intermediates **34a-d**.* Benzoyl isothiocyanate (547 µL, 4.07 mmol) was added dropwise to a solution of the appropriate aniline **33a-d** (3.70 mmol) in dry DCM (12 mL) and the mixture was stirred at room temperature for 12 h. The solvent of reaction was evaporated, the solid was dissolved in THF/NaOH 1N (1/1, 15 mL) and the mixture was refluxed for 2 h. Next, H_2O and ethyl acetate were added and the aqueous phase was extracted three times with ethyl acetate. The combined organic phases were dried over Na_2SO_4 and evaporated. Crystallization from ether afforded intermediates **34a-d**.

*1-phenylthiourea (**34a**).* Yield 72%. MS (ESI) $[M + H]^+$: 153.1 *m/z*. ^1H NMR (DMSO-d_6 300 MHz): δ 7.09-7.14 (m, 1H), 7.30-7.42 (m, 6H), 9.67 (s, 1H).

*1-(3-hydroxyphenyl)thiourea (**34b**).* Yield 74%. MS (ESI) $[M + H]^+$: 169.2 *m/z*. ^1H NMR (DMSO-d_6 300 MHz): δ 6.50-6.54 (m, 1H), 6.74-6.77 (m, 1H), 6.87-6.88 (m, 1H), 7.09 (t, 1H, J = 8.0 Hz), 7.32-7.36 (bs, 2H), 9.45 (s, 1H), 9.58 (s, 1H).

*1-(3-methoxyphenyl)thiourea (**34c**).* Yield 75%. MS (ESI) $[M + H]^+$: 183.3 *m/z*. ^{1}H NMR (DMSO-d_6 300 MHz): δ 3.74 (s, 3H), 6.67-6.70 (m, 1H), 6.90-6.94 (m, 1H), 7.11-7.13 (m, 1H), 7.22 (t, 1H, J = 8.1 Hz), 7.46-7.49 (bs, 2H), 9.73 (s, 1H).

*1-(4-acetylphenyl)thiourea (**34d**).* Yield 78%. MS (ESI) $[M + H]^+$: 195.4 *m/z*. ^{1}H NMR (DMSO-d_6 300 MHz): δ 2.49 (s, 3H), 7.79-7.83 (m, 2H), 7.87-8.03 (m, 4H), 10.69 (s, 1H).

*General Procedure for the Synthesis of Compounds **35a-d**.* A solution of intermediate **32** (50 mg, 0.18 mmol) and the proper thiourea **34a-d** (0.18 mmol) in ethanol (2.5 mL) was heated at reflux for 1 h. After cooling down to room temperature, saturated aqueous $NaHCO_3$ solution, H_2O and ethyl acetate were added and the aqueous phase was extracted three times with ethyl acetate. The combined organic phases were washed with brine, dried over Na_2SO_4 and concentrated under vacuum. The crude was purified by flash chromatography using DCM/MeOH (97/3) as eluent.

*N-(4'-methyl-2-(phenylamino)-[4,5'-bithiazol]-2'-yl)acetamide (**35a**).* Yield 85%; mp 187-189 °C. MS (ESI) $[M + H]^+$: 331.1 *m/z*. ^{1}H NMR ($CDCl_3$ 400 MHz): δ 2.19 (s, 3H), 2.57 (s, 3H), 6.58 (s, 1H), 7.10-7.12 (m, 1H), 7.36-7.42 (m, 4H), 8.18 (s, 1H), 11.94 (s, 1H). ^{13}C NMR ($CDCl_3$ 100.6 MHz): δ 17.00, 23.07, 102.63, 118.50 (2x), 121.29, 123.32, 129.54 (2x), 140.15, 142.70, 143.31, 156.66, 164.76, 167.92. Anal. ($C_{15}H_{14}N_4OS_2$) C, H, N.

*N-(2-((3-hydroxyphenyl)amino)-4'-methyl-[4,5'-bithiazol]-2'-yl)acetamide (**35b**).* Yield 71%; mp 148-149 °C. MS (ESI) $[M + H]^+$: 347.2 *m/z*. ^{1}H NMR (acetone- d_6 400 MHz): δ 2.26 (s, 3H), 2.51 (s, 3H), 6.52-6.54 (m, 1H), 6.78 (s, 1H), 7.15-7.18 (m, 2H), 7.27 (s, 1H), 8.45 (s, 1H), 9.30 (s, 1H), 10.85 (s, 1H). ^{13}C NMR (acetone- d_6 100.6 MHz): δ 16.51, 21.90, 101.85, 104.58, 108.75, 109.12, 120.91, 129.81, 142.39, 143.14, 143.95, 155.28, 158.21, 163.25, 167.72. Anal. ($C_{15}H_{14}N_4O_2S_2$) C, H, N.

*N-(2-((3-methoxyphenyl)amino)-4'-methyl-[4,5'-bithiazol]-2'-yl)acetamide (**35c**).* Yield 74%; mp 118-119 °C. MS (ESI) $[M + H]^+$: 361.2 *m/z*. ^{1}H NMR (DMSO-d_6 400 MHz): δ 2.14

(s, 3H), 2.48 (s, 3H), 3.82 (s, 3H), 6.53 (d, 1H, J = 8.2 Hz), 6.90 (s, 1H), 6.98 (s, 1H, J = 8.2 Hz), 7.20 (t, 1H, J = 8.2 Hz), 7.71 (s, 1H), 10.42 (s, 1H), 12.06 (s, 1H). ^{13}C NMR (DMSO-d_6 100.6 MHz): δ 17.53, 22.93, 55.52, 102.71, 105.60, 107.78, 109.65, 120.81, 130.02, 142.77, 142.90, 143.12, 155.59, 160.40, 162.96, 168.75. Anal. ($C_{16}H_{16}N_4O_2S_2$) C, H, N.

*N-(2-((4-acetylphenyl)amino)-4'-methyl-[4,5'-bithiazol]-2'-yl)acetamide (**35d**).* Yield 79%; mp 233-235 °C. MS (ESI) $[M + H]^+$: 373.2 *m/z*. ^{1}H NMR (DMSO-d_6 400 MHz): δ 2.15 (s, 3H), 2.51 (s, 3H), 2.54 (s, 3H), 7.07 (s, 1H), 7.77 (d, 2H, J = 8.7 Hz), 7.97 (d, 2H, J = 8.7 Hz), 10.79 (s, 1H), 12.11 (s, 1H). ^{13}C NMR (DMSO-d_6 100.6 MHz): δ 17.49, 22.93, 26.82, 104.38, 116.33 (2x), 120.33, 130.34, 130.42 (2x), 143.41, 145.48, 152.60, 155.63, 162.37, 168.83, 196.63. Anal. ($C_{17}H_{16}N_4O_2S_2$) C, H, N.

*Synthesis of 1-(3-acetylphenyl)guanidine (**36**).* Nitric acid (164 µL, 3.70 mmol) was added to a solution of 3'-aminoacetophenone **22** (500 mg, 3.70 mmol) in ethanol (10 mL), followed by addition of a solution of cyanamide (778 mg, 18.5 mmol) in a minimal amount of water. The mixture was heated at reflux for 24 h and concentrated in vacuum. After cooling to 0 °C, ether was added and the precipitate was separated by filtration over a Buchner funnel. Then saturated aqueous $NaHCO_3$ solution and ethyl acetate were added to the solid and the aqueous phase was extracted three times with ethyl acetate. The combined organic phases were washed with brine, dried over Na_2SO_4 and concentrated under vacuum to obtain compound **36**, used in the next step without any further purification. Yield 73%. MS (ESI) $[M + H]^+$: 178.2 *m/z*. ^{1}H NMR (DMSO-d_6 300 MHz): δ 2.57 (s, 3H), 7.49 (bs, 3H), 7.58-7.60 (m, 2H), 7.76-7.78 (m, 1H), 7.88 (s, 1H), 9.67 (bs, 1H).

*Synthesis of 1-(3-((4-(2-amino-4-methylthiazol-5-yl)-1H-imidazol-2-yl)amino)phenyl)ethanone (**37**).* A solution of intermediate **36** (150 mg, 0.85 mmol) in ethanol (5 mL) was added dropwise to a solution of compound **21** (200 mg, 0.85 mmol) and Et_3N (118 µL, 0.85 mmol) in ethanol (10 mL). The mixture was heated at reflux for 12 h,

after which H_2O and ethyl acetate were added. The organic phase was washed with saturated aqueous NH_4Cl solution and brine, dried over Na_2SO_4 and concentrated under vacuum to obtain compound **37**, used in the next step without any further purification. Yield 82%. MS (ESI) $[M + H]^+$: 314.3 *m/z*. ^{1}H NMR (DMSO-d_6 400 MHz): δ 2.37 (s, 3H), 2.64 (s, 3 H), 7.09 (s, 1 H), 7.65 (t, 1H, J = 7.9 Hz), 7.79 (d, 1H, J = 7.9 Hz), 7.94 (d, 1H, J = 7.9 Hz), 8.04 (s, 1H), 9.50 (bs, 2H), 10.56 (s, 1H), 12.01 (s, 1H).

*Synthesis of N-(5-(2-((3-acetylphenyl)amino)-1H-imidazol-4-yl)-4-methylthiazol-2-yl)acetamide (**38**).* Et_3N (89 µL, 0.64 mmol) was added to a stirred suspension of intermediate **37** (100 mg, 0.32 mmol) in dry DCM (4.5 mL) at 0 °C. After 15 minutes acetyl chloride (34 µL, 0.48 mmol), diluted in dry DCM (0.5 mL), was added dropwise. The resulting solution was warmed to room temperature and stirred for 8 h. Next, H_2O and DCM were added and the aqueous phase was extracted three times with DCM. The combined organic phases were washed with brine, dried over Na_2SO_4 and evaporated. The crude was purified by flash chromatography using DCM/MeOH (97/3) as eluent. Yield 47%; mp 222-225 °C. MS (ESI) $[M + H]^+$: 356.2 *m/z*. ^{1}H NMR (DMSO-d_6 400 MHz): δ 2.14 (s, 3H), 2.37 (s, 3H), 2.65 (s, 3H), 7.11 (s, 1H), 7.66 (t, 1H, J = 7.9 Hz), 7.79 (d, 1H, J = 7.9 Hz), 7.94 (d, 1H, J = 7.9 Hz), 8.05 (s, 1H), 10.56 (s, 1H), 11.84 (s, 1H), 12.06 (s, 1H). ^{13}C NMR (DMSO-d_6 100.6 MHz): δ 17.56, 22.56, 27.42, 116.75, 119.9, 120.51, 121.65, 127.71, 129.79, 138.10, 140.81, 143.21, 143.28, 154.98, 162.89, 168.63, 198.32. Anal. ($C_{17}H_{17}N_5O_2S$) C, H, N.

*Synthesis of 1-(3-acetylphenyl)-3-(3-nitrophenyl)thiourea (**40**).* 3'-aminoacetophenone **22** (300 mg, 2.22 mmol) was added to a solution of 3-nitrophenyl isothiocyanate (400 mg, 2.22 mmol) in dry DCM (6.50 mL). The solution was stirred at room temperature for 18 h. The precipitate was separated by filtration over a Buchner funnel and washed with ether, affording compound **40** as a white solid. Yield 88%. MS (ESI) $[M + H]^+$: 316.2 *m/z*. ^{1}H NMR (DMSO-d_6 400 MHz): δ 2.58 (s, 3H), 7.52 (t, 1H, J = 7.9 Hz), 7.63 (t, 1H, J = 8.1 Hz), 7.76-

7.78 (m, 2H), 7.92 (d, 1H, *J* = 7.9 Hz), 7.98 (d, 1H, *J* = 8.1 Hz), 8.07 (s, 1H), 8.56 (s, 1H), 10.31 (bs, 1H), 10.33 (bs, 1H).

*Synthesis of 1-(3-acetylphenyl)-3-(3-aminophenyl)thiourea (**41**).* Iron powder (1490 mg, 26.67 mmol), water (7 mL) and concentrated HCl (4 drops) were added to a solution of compound **40** (400 mg, 1.27 mmol) in ethanol (35 mL). After heating at reflux for 2 h, the mixture was filtrated hot, washed with ethanol and concentrated in vacuum. The crude was purified by flash chromatography using DCM/MeOH (98/2) as eluent. Yield 75%. MS (ESI) $[M + H]^+$: 286.1 *m/z*. ^{1}H NMR ($CDCl_3$ 400 MHz): δ 2.58 (s, 3H), 3.20-3.51 (bs, 2H), 6.59-6.62 (m, 2H), 6.68 (d, 1H, *J* = 7.7 Hz), 7.18 (t, 1H, *J* = 7.8 Hz), 7.45 (t, 1H, *J* = 7.8 Hz), 7.74-7.79 (m, 2H), 7.95 (s, 1H), 8.05 (s, 1H), 8.38 (s, 1H).

*General Procedure for the Synthesis of Compounds **42a,b**.* The proper acyl chloride (0.53 mmol) was added to a stirred solution of intermediate **41** (100 mg, 0.35 mmol) and pyridine (56 μL, 0.70 mmol) in dry THF (4 mL). The resulting solution was stirred at room temperature for 2 h, after which H_2O and ethyl acetate were added and the aqueous phase was extracted three times with ethyl acetate. The combined organic phases were washed with brine, dried over Na_2SO_4 and concentrated under vacuum. The crude was purified by flash chromatography using DCM/MeOH (99/1) as eluent.

*N-(3-(3-(3-acetylphenyl)thioureido)phenyl)acetamide (**42a**).* Yield 67%; mp 171-173 °C. MS (ESI) $[M + H]^+$: 328.1 *m/z*. ^{1}H NMR (DMSO-d_6 400 MHz): δ 2.04 (s, 3H), 2.57 (s, 3H), 7.16-7.19 (m, 1H), 7.25 (t, 1H, *J* = 7.9 Hz), 7.35-7.37 (m, 1H), 7.47 (t, 1H, *J* = 7.9 Hz), 7.71-7.79 (m, 3H), 8.07 (bs, 1H), 9.89 (s, 1H), 9.96 (s, 1H), 9.98 (s, 1H). ^{13}C NMR (DMSO-d_6 100.6 MHz): 23.43, 27.23, 116.20, 117.10, 119.38, 123.64, 124.55, 128.90, 128.98, 129.04, 136.97, 139.64, 140.17, 140.52, 168.56, 180.27, 197.97. Anal. ($C_{17}H_{17}N_3O_2S$) C, H, N.

*N-(3-(3-(3-acetylphenyl)thioureido)phenyl)pivalamide (**42b**).* Yield 69%; mp 157-159 °C. MS (ESI) $[M + H]^+$: 370.3 *m/z*. ^{1}H NMR (DMSO-d_6 300 MHz): δ 1.22 (s, 9H), 2.57 (s, 3H),

7.14 (d, 1H, *J* = 7.9 Hz), 7.25 (t, 1H, *J* = 7.9 Hz), 7.42-7.50 (m, 2H), 7.71-7.80 (m, 3H), 8.06 (bs, 1H), 9.25 (s, 1H), 9.89 (s, 1H), 9.94 (s, 1H). ^{13}C NMR (DMSO-d_6 100.6 MHz): δ 27.23, 27.65 (3x), 30.90, 116.29, 117.14, 119.35, 123.68, 124.71, 128.88, 128.92, 129.10, 137.43, 139.65, 140.20, 140.52, 176.96, 180.27, 197.97. Anal. ($C_{20}H_{23}N_3O_2S$) C, H, N.

*Synthesis of 1-(4-(dimethylamino)phenyl)thiourea (**44**)*. Benzoyl isothiocyanate (543 µL, 4.04 mmol) was added dropwise to a solution of N,N-Dimethyl-p-phenylenediamine **43** (500 mg, 3.67 mmol) in dry DCM (12 mL) and the mixture was stirred at room temperature for 12 h. The solvent of reaction was evaporated, the solid was dissolved in THF/NaOH 1N (1/1, 15 mL) and the mixture was refluxed for 3 h. Next, H_2O and ethyl acetate were added and the aqueous phase was extracted three times with ethyl acetate. The combined organic phases were dried over Na_2SO_4 and evaporated. The resulting solid was crystallized from ether. Yield 80%. MS (ESI) $[M + H]^+$: 196.4 *m/z*. ^{1}H NMR (DMSO-d_6 300 MHz): δ 2.88 (s, 6H), 6.69 (d, 2H, *J* = 8.7 Hz), 7.08 (d, 2H, *J* = 8.7 Hz), 7.55 (bs, 2H), 9.58 (s, 1H).

*Synthesis of N^2-(4-(dimethylamino)phenyl)-4'-methyl-[4,5'-bithiazole]-2,2'-diamine (**45**)*. Intermediates **21** (150 mg, 0.64 mmol) and **44** (125 mg, 0.64 mmol) were suspended in ethanol (6 mL) and the mixture was heated at reflux for 30 minutes. Then saturated aqueous $NaHCO_3$ solution and ethyl acetate were added to the mixture and the aqueous phase was extracted three times with ethyl acetate. The combined organic phases were washed with brine, dried over Na_2SO_4 and concentrated under vacuum. Ether was added to the crude and the solid obtained was filtered over a Buchner funnel, washed with ether and used in the following step without any further purification. Yield 77%. MS (ESI) $[M + H]^+$: 332.2 *m/z*. ^{1}H NMR (DMSO-d_6 400 MHz): δ 2.47 (s, 3H), 2.86 (s, 6H), 6.72 (s, 1H), 6.76 (d, 2H, *J* = 8.8 Hz), 7.43 (d, 2H, *J* = 8.8 Hz), 9.21 (bs, 2H), 10.58 (s, 1H).

*N-(2-((4-(dimethylamino)phenyl)amino)-4'-methyl-[4,5'-bithiazol]-2'-yl)propionamide (**46**)*. Et_3N (84 µL, 0.60 mmol) was added to a stirred suspension of intermediate **45** (100 mg,

0.30 mmol) in dry DCM (4 mL) at 0 °C. After 15 minutes propionyl chloride (39 μL, 0.45 mmol), diluted in dry DCM (0.5 mL), was added dropwise. The resulting solution was warmed to room temperature and stirred for 8 h. Next, H_2O and DCM were added and the aqueous phase was extracted twice with DCM. The combined organic phases were washed with brine, dried over Na_2SO_4 and evaporated. The crude was purified by flash chromatography using DCM/MeOH (98/2) as eluent. Yield 68%; mp 222-224 °C. MS (ESI) $[M + H]^+$: 388.3 *m/z*. ^{1}H NMR (DMSO-d_6 400 MHz): δ 1.10 (t, 3H, J = 7.6 Hz), 2.43 (q, 2H, J = 7.6 Hz), 2.47 (s, 3H), 2.86 (s, 6H), 6.73 (s, 1H), 6.76 (d, 2H, J = 8.8 Hz), 7.43 (d, 2H, J = 8.8 Hz), 9.90 (s, 1H), 11.98 (s, 1H). ^{13}C NMR (DMSO-d_6 100.6 MHz): δ 8.78, 16.88, 30.43, 40.46 (2x), 101.02, 113.74 (2x), 120.67 (2x), 121.44, 131.54, 143.10, 144.02, 147.72, 155.12, 165.29, 171.76. Anal. ($C_{18}H_{21}N_5OS_2$) C, H, N.

Biology

Antiviral assays – materials and methods Assay preparation

Enterovirus (EV):

Rhabdosarcoma (RD) cells, Vero cells and Hela-Rh cells, subcultured in cell growth medium [MEM Rega3 (Cat. N°19993013; Invitrogen) supplemented with 10% FCS (Integro), 5 ml 200 mM L-glutamine (25030024) and 5 mL 7.5% sodium bicarbonate (25080060)] at a ratio of 1:4 and grown for 7 days in 150 cm^2 tissue culture flasks (Techno Plastic Products), were harvested and seeded in a 96-well plate at a cell density of 20 000 cells/well in assay medium (MEM Rega3, 2% FCS, 5 ml L-glutamine and 5 ml sodium bicarbonate) to perform standardized antiviral assay against EV71 and EVD68, CV and PV, RV02 and RV14, respectively.

Antiviral activity and cytotoxicity determinations

Compounds were prepared as DMSO stock solution with a final compound concentration of 10mM. The compound profiling setup was performed employing a Freedom EVO200 liquid handling platform (Tecan). The evaluation of the cytostatic/cytotoxic as well as the antiviral effect of each compound was performed in parallel within one run. Three 8-step 1-to-5 dilution series were prepared (starting from 100 µM) in assay medium added to empty wells (picornaviruses: 96-well microtiter plates, Falcon, BD) or in the medium present on top of pre-seeded cells. Subsequently, 50 µL of a 4x virus dilution in assay medium (assay medium supplemented with 15 ml $MgCl_2$ 1M (Sigma, M1028) in case of RV) was added followed by 50 µL of cell suspension. The assay plates were returned to the incubator for 2-3 (picornavirus, 35°C for RV) days, a time at which maximal cytopathic effect (CPE) for picornaviruses is observed.

For the evaluation of cytostatic/cytotoxic effects and for the evaluation of the antiviral effect in case of PV, CV, RV, the assay medium was replaced with 75 µL of a 5% MTS (Promega) solution in phenol red-free medium and incubated for 1.5 hours (37°C, 5% CO_2, 95-99% relative humidity). Absorbance was measured at a wavelength of 498 nm (Safire2, Tecan) and optical densities (OD values) were converted to percentage of untreated controls.

Analysis of the raw data, quality control of each individual dose-response curve and calculation, if possible, of the EC_{50}, EC_{90} and CC_{50} values was performed employing ViroDM, a custom-made data processing software package. The EC_{50} and EC_{90} (values derived from the dose-response curve) represent the concentrations at which respectively 50% and 90% inhibition of viral replication would be observed. The CC_{50} (value derived from the dose-response curve) represents the concentration at which the metabolic activity of the cells would be reduced to 50 % of the metabolic activity of untreated cells.

The EC_{50}, EC_{90} and CC_{50} ± SD were, whenever possible, calculated respectively as the median of all the EC_{50}, EC_{90} or CC_{50} values derived from the 3 individual dose-response curves. The selectivity index (SI), indicative of the therapeutic window of the compound, was calculated as CC_{50}/EC_{50}. No further statistical analysis was performed.

CFTR assays

The effects of compounds on CFTR biogenesis and function were measured using newly developed assays exploiting CFTR fusion probes with anion-sensitive YFP[61] and pH-sensitive pHTomato.[62] Lipofectamine transfection was used for transient transfection of HEK293 cells. Cells plated in 96-well plates were incubated with the YFP-CFTR- or CFTR-pHTomato- encoding plasmid[48] using Lipofectamine 2000 (Life Technologies), according to manufacturer's instructions. Following transfection, cell plates were returned to the 37°C incubator for 24 h. Plates were further incubated at 30°C for 24 h prior to imaging, with or without additional drug treatment.

All imaging was carried out using ImageXpress (ImageXpress Micro XLS, Molecular Devices); an image-acquisition system equipped with wide-field inverted fluorescence microscope and fluidics robotics. Images were obtained with a 20X objective, using excitation/emission filters 472 ± 30 nm and 520 ± 35 nm, for YFP-CFTR and 531 ± 20 nm and 592 ± 20 nm for CFTR-pHTomato. In the latter assay, eGFP and Hoechst nuclear stain images were also acquired for each well, using excitation/emission filters 472 ± 30 nm and 520 ± 35 nm, and 377 ± 25 nm and 447 ± 30 nm, respectively. For each plate, the laser intensity and exposure were optimized to achieve the highest possible fluorescence whilst avoiding both photobleaching and saturation (illumination intensity 100-150/225 cd, and exposure 0.1 – 0.2 s)

For the YFP-CFTR assays, before imaging, cells were washed twice with 100 µl standard buffer (140 mM NaCl, 4.7 mM KCl, 1.2 mM $MgCl_2$, 5 mM HEPES, 2.5 mM $CaCl_2$, 1 mM Glucose, pH 7.4). Images were taken for 150 s at a frequency of 0.5 Hz. 50 µL extracellular I^- (as standard buffer with 140 mM NaCl replaced with 300 mM NaI; resulting in 100 mM final [I^-]) was added at 20 s, and activating compounds (50 µM Forskolin alone or together with 10 µM compounds for acute treatment) were added at 60 s.

For the CFTR-pHTomato assay, before imaging, cells were washed twice with 100 µL standard buffer (as above). During imaging, extracellular pH was changed using addition of 50 µL pH 6 buffer (as standard buffer, with 5 mM HEPES replaced with 10 mM MES: final [MES] 3.3 mM, ~ pH 6.5), and 50 µL pH 9 buffer (as standard buffer, with 5 mM HEPES replaced with 100 mM Tris: final [Tris] 25 mM, ~ pH 8.8). Two pHTomato images (acquisition frequency 0.5 Hz) were taken in each condition. To account for variation in transfection efficiency the pHTomato fluorescence was normalized using average fluorescence intensity of a soluble eGFP, co-expressed in the cytosol. Because the rise in pHTomato fluorescence falls largely within the 6.5 to 8.8 pH range,[63] the change in fluorescence obtained upon increasing extracellular pH ($\Delta F_{membrane}$) was used as an estimate of membrane-exposed CFTR.

In vitro kinase inhibition assays

Recombinant full length, HIS6-tagged PI4KIIIβ was purchased from ProQinase (Germany); recombinant full length, GST tagged PI4KIIIα was from Life Technologies. Recombinant full length, HIS6-tagged (PI3K-α) and full length, myc-tagged (p85α) PI3K-α/p85α was purchased from ProQinase (Germany).

Assay conditions:

PI4KIIIβ, PI4KIIIα and PI3K- α/p85α reactions were performed in 10 µL using 20 mM Tris-HCl pH 7.5, 0.125 mM EGTA, 2 mM DTT, 0.04% Triton, 3 mM $MgCl_2$, 3 mM $MnCl_2$, 20 µM ATP, 0.01 µCi γ-P33 ATP, 200 µM Pi:3PS, 10% DMSO, 0.4 ng/µL of PI4KIIIβ, 16 ng/µL of PI4KIIIα and 7.6 ng/µL of PI3K- α/p85α. All reactions were performed at 30 °C for 10 min. Reactions were stopped by adding 5µL of phosphoric acid 0.8%. Aliquots (10 µL) were then transferred into a P30 Filtermat (PerkinElmer), washed five times with 0.5 % phosphoric acid and four times with water for 5 min. The filter was dried and transferred to a sealable plastic bag, and scintillation cocktail (4 mL) was added. Spotted reactions were read in a scintillation counter (Trilux, Perkinelmer). IC_{50} values were obtained according to Equation (1), where v is the measured reaction velocity, V is the apparent maximal velocity in the absence of inhibitor, I is the inhibitor concentration, and IC_{50} is the 50% inhibitory concentration.

$$v = V/\{1+(I/IC_{50})\} \quad (1)$$

Lipidic substrate preparation:

PI: phosphatidylinositol (Sigma); PS: 2-Oleoyl-1-palmitoyl-sn-glycero-3-phospho-L-serine (Sigma). PI and PS were dissolved in chloroform/methanol 9:1 and mixed at a 1:3 ratio. After chloroform/methanol evaporation, water was added to 1:62.5 w/v and the mixture sonicated to clarity.

Kinase Panel:

All Tyrosine- and Serine/Threonine kinase reactions were performed according to manufacturer's instructions, using 10-50 ng of enzyme. Details on the nature of the substrates and their concentration are reported elsewhere.[63] For some kinases, NP-40 or BSA was added. All reactions were performed in 10 µL at 30 °C for 10 min using protein low-binding

tubes. Reactions were stopped, transferred to filter and counted as reported in Ref. 59. PI4KIIIβ was purchased from Proqinase. Reactions were performed according to the manufacturer's instructions and detected using ADP-Glo™ Lipid Kinase Assay (Promega).

Supporting Information. 3D coordinates of the PI4KIIIβ and PI4KIIIα homology models. Molecular formula strings. This material is available free of charge via the Internet at http://pubs.acs.org.

AUTHOR INFORMATION

Corresponding Author

*Prof. Marco Radi, P4T Group, Dipartimento di Scienze degli Alimenti e del Farmaco, Università degli Studi di Parma, Viale delle Scienze, 27/A, 43124 Parma, Italy. E-mail: marco.radi@unipr.it; phone: +39 0521 906080; fax: +39 0521 905006

*Prof. Johan Neyts, Laboratory of Virology and Experimental Chemotheraphy, Rega Institute for Medical Research, KU Leuven, Minderbroedersstraat 10, 3000, Leuven, Belgium. E-mail: johan.neyts@kuleuven.be; phone: +32 163 21893; fax: +32 163 37340

Author Contributions

The manuscript was written through contributions of all authors. All authors have given approval to the final version of the manuscript.

ACKNOWLEDGMENT

Work in the P4T group has been supported by the Chiesi Foundation (Bando Dottorati di Ricerca 2014) and by the University of Parma (to MR). Work in the IGM laboratory has been supported by the Italian Cancer Research Association (AIRC), Grant IG15868. EL's work was supported by the Cystic Fibrosis Trust, (CFT Project No RS31). SL is funded by the

China Scholarship Council (CSC) (Grant 201403250056) and KL is supported by the European Union as a Marie-Sklodowska Curie European Training Network ANTIVIRALS (GA 642434).

ABBREVIATIONS

CF, cystic fibrosis; CFTR, cystic fibrosis transmembrane conductance regulator; COPD, chronic obstructive pulmonary disorder; CPE, cytopathic effect; CVB3, coxsackievirus B3; DC-SIGN, dendritic cell-specific intercellular adhesion molecule-3 grabbing nonintegrin; ECHO11, Echovirus 11; EV, enterovirus; F508del, deletion of Phe 508; RV, human rhinovirus; HTD, high-throughput docking; PI, phosphatidylinositol; PI4K, phosphatidylinositol 4-kinase; PIP_2, phosphatidylinositol 4,5-bisphosphate; PIP_3, phosphatidylinositol 3,4,5-trisphosphate; PI4P, phosphatidylinositol 4-phosphate; PV1, poliovirus 1; TGN, trans-Golgi network.

REFERENCES

(1) Adams, M. J.; King, A. M. Q.; Carstens, E. B. Ratification Vote on Taxonomic Proposals to the International Committee on Taxonomy of Viruses (2013). *Arch. Virol.* **2013**, *158*, 2023–2030.

(2) Tapparel, C.; Siegrist, F.; Petty, T. J.; Kaiser, L. Picornavirus and Enterovirus Diversity with Associated Human Diseases. *Infect. Genet. Evol.* **2013**, *14*, 282-293.

(3) Sabanathan, S.; Tan, L. V.; Thwaites, L.; Wills, B.; Qui, P. T.; Rogier van Doorn, H. Enterovirus 71 Related Severe Hand, Foot and Mouth Disease Outbreaks in South-East Asia: Current Situation and Ongoing Challenges. *J. Epidemiol. Community Health* **2014**, *68*, 500-502.

(4) Esposito, S.; Bosis, S.; Niesters, H.; Principi, N. Enterovirus D68 Infection. *Viruses* **2015**, *7*, 6043-6050.

(5) Leigh, R.; Proud, D. Virus-Induced Modulation of Lower Airway Diseases: Pathogenesis and Pharmacologic Approaches to Treatment. *Pharmacol. Ther.* **2015**, *148*, 185-198.

(6) Wat, D. Impact of Respiratory Viral Infections on Cystic Fibrosis. *Postgrad. Med. J.* **2003**, *79*, 201-203.

(7) (a) Waters, V.; Ratjen, F. Pulmonary Exacerbations in Children with Cystic Fibrosis. *Ann. Am. Thorac. Soc.* **2015**, *12* (Suppl. 2), S200-S206. (b) Singanayagam, A.; Joshi, P. V.; Mallia, P.; Johnston, S. L. Viruses Exacerbating Chronic Pulmonary Disease: The Role of Immune Modulation. *BMC Med.* **2012**, *10*, 27. (c) Goffard, A.; Lambert, V.; Salleron, J.; Herwegh, S.; Engelmann, I.; Pinel, C.; Pin, I.; Perrez, T.; Prévotat, A.; Dewilde, A.; Delhaes, L. Virus and Cystic Fibrosis: Rhinoviruses Are Associated with Exacerbations in Adult Patients. *J. Clin. Virol.* **2014**, *60*, 147-153. (d) Esther, C. R.; Lin, F. C.; Kerr, A.; Miller, M. B.; Gilligan, P. H. Respiratory Viruses Are Associated with Common Respiratory Pathogens in Cystic Fibrosis. *Pediatr. Pulmonol.* **2014**, *49*, 926–931.

(8) van Ewijk, B. E.; van der Zalm, M. M.; Wolfs, T. F. W.; Fleer, A.; Kimpen, J. L. L.; Wilbrink, B.; van der Ent, C. K. Prevalence and Impact of Respiratory Viral Infections in Young Children With Cystic Fibrosis: Prospective Cohort Study. *Pediatrics* **2008**, *122*, 1171-1176.

(9) Debing, Y.; Neyts, J.; Delang, L. The Future of Antivirals: Broad-Spectrum Inhibitors. *Curr. Opin. Infect. Dis.* **2015**, *28*, 596-602.

(10) de Chassey, B.; Meyniel-Schicklin, L.; Aublin-Gex, A.; André, P.; Lotteau, V. New Horizons for Antiviral Drug Discovery from Virus-Host Protein Interaction Networks. *Curr. Opin. Virol*. **2012**, *2*, 606-613.

(11) Delang, L.; Paeshuyse, J.; Neyts, J. The Role of Phosphatidylinositol 4-Kinases and Phosphatidylinositol 4-Phosphate during Viral Replication. *Biochem. Pharmacol.* **2012**, *84*, 1400-1408.

(12) Hsu, N. Y.; Ilnytska, O.; Belov, G.; Santiana, M.; Chen, Y. H.; Takvorian, P. M.; Pau, C.; van der Schaar, H.; Kaushik-Basu, N.; Balla, T.; Cameron, C. E.; Ehrenfeld, E.; van Kuppeveld, F. J. M.; Altan-Bonnet, N. Viral Reorganization of the Secretory Pathway Generates Distinct Organelles for RNA Replication. *Cell* **2010**, *141*, 799-811.

(13) Arita, M.; Kojima, H.; Nagano, T.; Okabe, T.; Wakita, T.; Shimizu, H. Phosphatidylinositol 4-kinase III Beta Is a Target of Enviroxime-Like Compounds for Antipoliovirus Activity. *J. Virol.* **2011**, *85*, 2364-2372.

(14) van der Schaar, H. M.; Leyssen, P.; Thibaut, H. J.; de Palma, A.; van der Linden, L.; Lanke, K. H. W.; Lacroix, C.; Verbeken, E.; Conrath, K.; MacLeod, A. M.; Mitchell, D. R.; Palmer, N. J.; van de Poël, H.; Andrews, M.; Neyts, J.; van Kuppeveld, F. J. M. A Novel, Broad-Spectrum Inhibitor of Enterovirus Replication That Targets Host Cell Factor Phosphatidylinositol 4-Kinase IIIβ. *Antimicrob. Agents Chemother.* **2013**, *57*, 4971-4981.

(15) Di Paolo, G.; De Camilli, P. Phosphoinositides in Cell Regulation and Membrane Dynamics. *Nature* **2006**, *443*, 651-657.

(16) Clayton, E. L.; Minogue, S.; Waugh, M. G. Mammalian Phosphatidylinositol 4-Kinases as Modulators of Membrane Trafficking and Lipid Signaling Networks. *Prog. Lipid Res.* **2013**, *52*, 294-304.

(17) Balla, T. Phosphoinositides: Tiny Lipids With Giant Impact on Cell Regulation. *Physiol. Rev*. **2013**, *93*, 1019-1137.

(18) Himmel, B.; Nagel, G. Protein Kinase-Independent Activation of CFTR by Phosphatidylinositol Phosphates. *EMBO Rep.* **2004**, *5*, 85-90.

(19) Balla, A.; Balla, T. Phosphatidylinositol 4-Kinases: Old Enzymes with Emerging Functions. *Trends Cell Biol.* **2006**, *16*, 351-361.

(20) Altan-Bonnet, N.; Balla, T. Phosphatidylinositol 4-Kinases: Hostages Harnessed to Build Panviral Replication Platforms. *Trends Biochem. Sci.* **2012**, *37*, 293-302.

(21) Boura, E.; Nencka, R. Phosphatidylinositol 4-Kinases: Function, Structure, and Inhibition. *Exp. Cell Res.* **2015**, *337*, 136-145.

(22) Mejdrová, I.; Chalupská, D.; Kögler, M.; Šála, M.; Plačková, P.; Baumlová, A.; Hřebabecký, H.; Procházková, E.; Dejmek, M.; Guillon, R.; Strunin, D.; Weber, J.; Lee, G.; Birkus, G.; Mertlíková-Kaiserová, H.; Boura, E.; Nencka, R. Highly Selective Phosphatidylinositol 4-Kinase IIIβ Inhibitors and Structural Insight into Their Mode of Action. *J. Med. Chem.* **2015**, *58*, 3767-3793.

(23) MacLeod, A. M.; Mitchell, D. R.; Palmer, N. J.; Van de Poël, H.; Conrath, K.; Andrews, M.; Leyssen, P.; Neyts, J. Identification of a Series of Compounds with Potent Antiviral Activity for the Treatment of Enterovirus Infections. *ACS Med. Chem. Lett.* **2013**, *4*, 585-589.

(24) LaMarche, M. J.; Borawski, J.; Bose, A.; Capacci-Daniel, C.; Colvin, R.; Dennehy, M.; Ding, J.; Dobler, M.; Drumm, J.; Gaither, L. A.; Gao, J.; Jiang, X.; Lin, K.; McKeever, U.; Puyang, X.; Raman, P.; Thohan, S.; Tommasi, R.; Wagner, K.; Xiong, X.; Zabawa, T.; Zhu, S.; Wiedmann, B. Anti-Hepatitis C Virus Activity and Toxicity of Type III Phosphatidylinositol-4-Kinase Beta Inhibitors. *Antimicrob. Agents Chemother.* **2012**, *56*, 5149-5156.

(25) Balla, A.; Tuymetova, G.; Toth, B.; Szentpetery, Z.; Zhao, X.; Knight, Z. A.; Shokat, K.; Steinbach, P. J.; Balla, T. Design of Drug-Resistant Alleles of Type-III Phosphatidylinositol 4-Kinases Using Mutagenesis and Molecular Modeling. *Biochemistry* **2008**, *47*, 1599-1607.

(26) Knight, Z. A.; Gonzalez, B.; Feldman, M. E.; Zunder, E. R.; Goldenberg, D. D.; Williams, O.; Loewith, R.; Stokoe, D.; Balla, A.; Toth, B.; Balla, T.; Weiss, W. A.; Williams, R. L.; Shokat, K. M. A Pharmacological Map of the PI3-K Family Defines a Role for p110alpha in Insulin Signaling. *Cell* **2006**, *125*, 733-747.

(27) Anighoro, A.; Bajorath, J.; Rastelli, G. Polypharmacology: Challenges and Opportunities in Drug Discovery: Miniperspective. *J. Med. Chem.* **2014**, *57*, 7874-7887.

(28) Reddy, A. S.; Zhang, S. Polypharmacology: Drug Discovery for the Future. *Expert Rev. Clin. Pharmacol.* **2013**, *6*, 41-47.

(29) Bowers, K. J.; Chow, E.; Xu, H.; Dror, R. O.; Eastwood, M. P.; Gregersen, B. A.; Klepeis, J. L.; Kolossvary, I.; Moraes, M. A.; Sacerdoti, F. D.; Salmon, J. K.; Shan, Y.; Shaw, D. E. Scalable Algorithms for Molecular Dynamics Simulations on Commodity Clusters. Proceedings of the 2006 ACM/IEEE conference on Supercomputing; ACM: New York, 2006.

(30) Wang, Y.; Suzek, T.; Zhang, J.; Wang, J.; He, S.; Cheng, T.; Shoemaker, B. A.; Gindulyte, A.; Bryant, S. H. PubChem BioAssay: 2014 update. *Nucleic Acids Res.* **2014**, *42* (Database issue), D1075-1082.

(31) http://www.asinex.com/ accessed on February 14, 2014.

(32) Pedemonte, N.; Sonawane, N. D.; Taddei, A.; Hu, J.; Zegarra-Moran, O.; Suen, Y. F.; Robins, L. I.; Dicus, C. W.; Willenbring, D.; Nantz, M. H.; Kurth, M. J.; Galietta, L. J.;

Verkman, A. S. Phenylglycine and Sulfonamide correctors of Defective Delta F508 and G551D Cystic Fibrosis Transmembrane Conductance Regulator Chloride-Channel Gating. *Mol. Pharmacol.* **2005**, *67*, 1797-1807.

(33) Pedemonte, N.; Lukacs, G. L.; Du, K.; Caci, E.; Zegarra-Moran, O.; Galietta, L. J.; Verkman, A. S. Small-molecule Correctors of Defective DeltaF508-CFTR Cellular Processing Identified by High-Throughput Screening. *J. Clin. Invest.* **2005**, *115*, 2564-2571.

(34) Burke, J. E.; Inglis, A. J.; Perisic, O.; Masson, G. R.; McLaughlin, S. H.; Rutaganira, F.; Shokat, K. M.; Williams, R. L. Structures of PI4KIIIβ Complexes Show Simultaneous Recruitment of Rab11 and Its Effectors. *Science* **2014**, *344*, 1035-1038.

(35) Yoo, C. L.; Yu, G. J.; Yang, B.; Robins, L. I.; Verkman, A. S.; Kurth, M. J. 4'-Methyl-4,5'-Bithiazole-Based Correctors of Defective ΔF508-CFTR Cellular Processing. *Bioorg. Med. Chem. Lett.* **2008**, *18*, 2610-2614.

(36) Donald, M. B.; Rodriguez, K. X.; Shay, H.; Phuan, P. W.; Verkman, A. S.; Kurth, M. J. Click-Based Synthesis of Triazolobithiazole ΔF508-CFTR Correctors for Cystic Fibrosis. *Bioorg. Med. Chem.* **2012**, *20*, 5247-5253.

(37) Haydon, D. J.; Bennett, J. M.; Brown, D.; Collins, I.; Galbraith, G.; Lancett, P.; Macdonald, R.; Stokes, N. R.; Chauhan, P. K.; Sutariya, J. K.; Nayal, N.; Srivastava, A.; Beanland, J.; Hall, R.; Henstock, V.; Noula, C.; Rockley, C.; Czaplewski, L. Creating an Antibacterial with in Vivo Efficacy: Synthesis and Characterization of Potent Inhibitors of the Bacterial Cell Division Protein FtsZ with Improved Pharmacological Properties. *J. Med. Chem.* **2010**, *53*, 3927-3936.

(38) De Lucca, G. V.; Kim, U. T.; Vargo, B. J.; Duncia, J. V.; Santella, J. B.; Gardner, D. S.; Zheng, C.; Liauw, A.; Wang, Z.; Emmett, G.; Wacker, D. A.; Welch, P. K.; Covington,

M.; Stowell, N. C.; Wadman, E. A.; Das, A. M.; Davies, P.; Yeleswaram, S.; Graden, D. M.; Solomon, K. A.; Newton, R. C.; Trainor, G. L.; Decicco, C. P.; Ko, S. S. Discovery of CC Chemokine Receptor-3 (CCR3) Antagonists with Picomolar Potency. *J. Med. Chem.* **2005**, *48*, 2194-2211.

(39) Diab, S.; Teo, T.; Kumarasiri, M.; Li, P.; Yu, M.; Lam, F.; Basnet, S. K. C.; Sykes, M. J.; Alberecht, H.; Milne, R.; Wang, S. Discovery of 5-(2-(Phenylamino)pyrimidin-4-yl)thiazol-2(3*H*)-one Derivatives as Potent Mnk2 Inhibitors: Synthesis, SAR Analysis and Biological Evaluation. *ChemMedChem* **2014**, *9*, 962-972.

(40) Sperandio, O.; Petitjean, M.; Tuffery, P. wwwLigCSRre: a 3D Ligand-Based Server for Hit Identification and Optimization. *Nucleic Acids Res*. **2009**, 37 (Web Server), W504-W509.

(41) (a) Radi, M.; Falchi, F.; Garbelli, A.; Samuele, A.; Bernardo, V.; Paolucci, S.; Baldanti, F.; Schenone, S.; Manetti, F.; Maga, G.; Botta, M. Discovery of the First Small Molecule Inhibitor of Human DDX3 Specifically Designed to Target the RNA Binding Site: Towards the next Generation HIV-1 Inhibitors. *Bioorg. Med. Chem. Lett.* **2012**, *22*, 2094-2098. (b) Bloom, J. D.; Digrandi, M. J.; Dushin, R. G.; Curran, K. J.; Ross, A. A.; Norton, E. B.; Terefenko, E.; Jones, T. R.; Feld, B.; Lang, S. A. Thiourea Inhibitors of Herpes Viruses. Part 1: Bis-(Aryl)thiourea Inhibitors of CMV. *Bioorg. Med. Chem. Lett.* **2003**, *13*, 2929–2932.

(42) Borrok, M. J.; Kiessling, L. Non-Carbohydrate Inhibitors of the Lectin DC-SIGN. *J. Am. Chem. Soc.* **2007**, *129*, 12780-12785.

(43) Ren, X. X.; Ma, L.; Liu, Q. W.; Li, C.; Huang, Z.; Wu, L.; Xiong, S. D.; Wang, J. H.; Wang, H. B. The Molecule of DC-SIGN Captures Enterovirus 71 and Confers Dendritic Cell-Mediated Viral Trans-Infection. *Virol. J.* **2014**, *11*, 47.

(44) Ye, L.; Hu, B.; El-Badri, F.; Hudson, B. M.; Phuan, P. W.; Verkman, A. S.; Tantillo, S. J.; Kurth, M. J. ΔF508-CFTR Correctors: Synthesis and Evaluation of Thiazole-Tethered Imidazolones, Oxazoles, Oxadiazoles, and Thiadiazoles. *Bioorg. Med. Chem. Lett.* **2014**, *24*, 5840-5844.

(45) Ford Siltz, L. A.; Viktorova, E. G.; Zhang, B.; Kouiavskaia, D.; Dragunsky, E.; Chumakov, K.; Isaacs, L.; Belov, G. A. New Small-Molecule Inhibitors Effectively Blocking Picornavirus Replication. *J. Virol.* **2014**, *88*, 11091-11107.

(46) Leong, W. F.; Chow, V. T. Transcriptomic and Proteomic Analyses of Rhabdomyosarcoma Cells Reveal Differential Cellular Gene Expression in Response to Enterovirus 71 Infection. *Cell. Microbiol.* **2006**, *8*, 565-580.

(47) Van Goor, F.; Hadida, S.; Grootenhuis, P. D. J.; Burton, B.; Stack, J. H.; Straley, K. S.; Decker, C. J.; Miller, M.; McCartney, J.; Olson, E. R.; Wine, J. J.; Frizzell, R. A.; Ashlock, M.; Negulescua, P. A. Correction of the F508del-CFTR Protein Processing Defect in Vitro by the Investigational Drug VX-809. *Proc. Natl. Acad. Sci. U. S. A.* **2011**, *108,* 18843–18848.

(48) Langron, E.; Simone, M. I.; Delalande, C. M. S.; Reymond,J.-L.; Selwood, D. L.; Vergani, P. Improved Fluorescence Assays to Measure the Defects Associated with F508del-CFTR Allow Identification of New Active Compounds. *Br. J. Pharmacol.* doi: 10.1111/bph.13715.

(49) Van Goor, F.; Hadida, S.; Grootenhuis, P. D. J.; Burton, B.; Cao, D.; Neuberger, T.; Turnbull, A.; Singh, A.; Joubran, J.; Hazlewood, A.; Zhou, J.; McCartney, J.; Arumugam, V.; Decker, C.; Yang, J.; Young, C.; Olson, E. R.; Wine, J. J.; Frizzell, R. A.; Ashlock, M.; Negulescu, P. Rescue of CF Airway Epithelial Cell Function in Vitro by a CFTR Potentiator, VX-770. *Proc. Natl. Acad. Sci. U. S. A.* **2009**, *106*, 18825–18830.

(50) Friesner, R. A.; Banks, J. L.; Murphy, R. B.; Halgren, T. A.; Klicic, J. J.; Mainz, D. T.; Repasky, M. P.; Knoll, E. H.; Shaw, D. E.; Shelley, M.; Perry, J. K.; Francis, P.; Shenkin, P. S. Glide: A New Approach for Rapid, Accurate Docking and Scoring. 1. Method and Assessment of Docking Accuracy. *J. Med. Chem.* **2004**, *47*, 1739–1749.

(51) Warren, G. L.; Andrews, C. W.; Capelli, A.-M.; Clarke, B.; LaLonde, J.; Lambert, M. H.; Lindvall, M.; Nevins, N.; Semus, S. F.; Senger, S.; Tedesco, G.; Wall, I. D.; Woolven, J. M.; Peishoff, C. E.; Head, M. S. A Critical Assessment of Docking Programs and Scoring Functions. *J. Med. Chem.* **2006**, *49*, 5912–5931.

(52) Manetti, F.; Falchi, F.; Crespan, E.; Schenone, S.; Maga, G.; Botta, M. N-(Thiazol-2-Yl)-2-Thiophene Carboxamide Derivatives as Abl Inhibitors Identified by a Pharmacophore-Based Database Screening of Commercially Available Compounds. *Bioorg. Med. Chem. Lett.* **2008**, *18*, 4328–4331.

(53) Jacobson, M. P.; Pincus, D. L.; Rapp, C. S.; Day, T. J. F.; Honig, B.; Shaw, D. E.; Friesner, R. A. A Hierarchical Approach to All-Atom Protein Loop Prediction. *Proteins: Struct. Funct. Bioinf.* **2004**, *55*, 351-367.

(54) Bates, P. A.; Kelley, L. A.; MacCallum, R. M.; Sternberg, M. J. E. Enhancement of Protein Modeling by Human Intervention in Applying the Automatic Programs 3D-JIGSAW and 3D-PSSM. *Proteins: Struct. Funct. Bioinf.* **2001**, Suppl. 5, 39-46.

(55) *Schrödinger Release 2014-3: Maestro*, version 9.9, Schrödinger, LLC, New York, NY, 2014.

(56) Irwin, J. J.; Sterling, T.; Mysinger, M. M.; Bolstad, E. S.; Coleman, R. G. ZINC: a Free Tool to Discover Chemistry for Biology. *J. Chem. Inf. Model.* **2012**, *52*, 1757-1768.

(57) *Schrödinger Release 2015-4: LigPrep*, version 3.6, Schrödinger, LLC, New York, NY, 2015.

(58) (a) *Schrödinger Release 2015-4: Schrödinger Suite 2015-4 Protein Preparation Wizard*; Epik version 3.4, Schrödinger, LLC, New York, NY, 2015; (b) Impact version 6.9, Schrödinger, LLC, New York, NY, 2015; Prime version 4.2, Schrödinger, LLC, New York, NY, 2015.

(59) Harder, E.; Damm, W.; Maple, J.; Wu, C.; Reboul, M.; Xiang, J.Y.; Wang, L.; Lupyan, D.; Dahlgren, M.K.; Knight, J.L.; Kaus, J.W.; Cerutti, D.S.; Krilov, G.; Jorgensen, W.L.; Abel, R.; Friesner, R.A. OPLS3: A Force Field Providing Broad Coverage of Drug-like Small Molecules and Proteins. *J. Chem. Theory Comput.* **2016**, *12*, 281-296.

(60) *Small-Molecule Drug Discovery Suite 2015-4: Glide*, version 6.9, Schrödinger, LLC, New York, NY, 2015.

(61) Galietta, L. J. V.; Haggie, P. M.; Verkman, A. S. Green Fluorescent Protein-Based Halide Indicators with Improved Chloride and Iodide Affinities. *FEBS Lett.* **2001**, *499*, 220-224.

(62) Li, Y.; Tsien, R. W. pHTomato, a Red, Genetically Encoded Indicator That Enables Multiplex Interrogation of Synaptic Activity. *Nat. Neurosci.* **2012**, *15*, 1047-1053.

(63) Tassini, S.; Castagnolo,D.; Scalacci, N.; Kissova, M.; Armijos-Rivera, J.I.; Giagnorio, F.; Maga, G.; Costantino, G.; Crespan, E.; Radi, M. A multicomponent pharmacophore fragment-decoration approach to identify selective LRRK2-targeting probes. *Med. Chem. Commun.* **2016**, *7*, 484-494.

Table of Contents Graphic